

Review

# Advances in Chirality Sensing with Macrocyclic Molecules

Xiaotong Liang<sup>1</sup>, Wenting Liang<sup>2</sup>, Pengyue Jin<sup>1</sup>, Hongtao Wang<sup>1,\*</sup>, Wanhua Wu<sup>1</sup> and Cheng Yang<sup>1,\*</sup>

<sup>1</sup> Key Laboratory of Green Chemistry & Technology of Ministry of Education, College of Architecture and Environment, Sichuan University, Chengdu 610064, China; liangxt598@stu.scu.edu.cn (X.L.); 2020223055124@stu.scu.edu.cn (P.J.); wuwanhua@scu.edu.cn (W.W.)

<sup>2</sup> Department of Chemistry, Institute of Environmental Science, Shanxi University, Taiyuan 030006, China; liangwt@sxu.edu.cn

\* Correspondence: wanght@scu.edu.cn (H.W.); yangchengyc@scu.edu.cn (C.Y.)

**Abstract:** The construction of chemical sensors that can distinguish molecular chirality has attracted increasing attention in recent years due to the significance of chiral organic molecules and the importance of detecting their absolute configuration and chiroptical purity. The supramolecular chirality sensing strategy has shown promising potential due to its advantages of high throughput, sensitivity, and fast chirality detection. This review focuses on chirality sensors based on macrocyclic compounds. Macrocyclic chirality sensors usually have inherent complexing ability towards certain chiral guests, which combined with the signal output components, could offer many unique advantages/properties compared to traditional chiral sensors. Chirality sensing based on macrocyclic sensors has shown rapid progress in recent years. This review summarizes recent advances in chirality sensing based on both achiral and chiral macrocyclic compounds, especially newly emerged macrocyclic molecules.

**Keywords:** chiral sensors; supramolecular; macrocycle; CD; CPL



**Citation:** Liang, X.; Liang, W.; Jin, P.; Wang, H.; Wu, W.; Yang, C. Advances in Chirality Sensing with Macrocyclic Molecules. *Chemosensors* **2021**, *9*, 279. <https://doi.org/10.3390/chemosensors9100279>

Academic Editor: Elena Benito Peña

Received: 12 August 2021

Accepted: 15 September 2021

Published: 29 September 2021

**Publisher's Note:** MDPI stays neutral with regard to jurisdictional claims in published maps and institutional affiliations.



**Copyright:** © 2021 by the authors. Licensee MDPI, Basel, Switzerland. This article is an open access article distributed under the terms and conditions of the Creative Commons Attribution (CC BY) license (<https://creativecommons.org/licenses/by/4.0/>).

## 1. Introduction

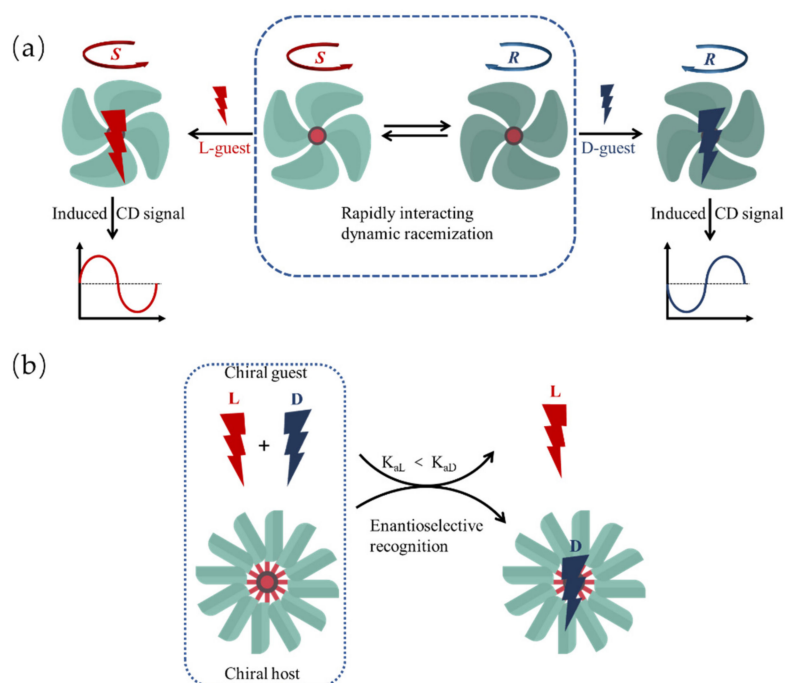
Chirality is a fundamental property of nature. Chiral molecules not only compose essential and fundamental components of living systems but could find wide applications in real life, such as in the pharmaceutical industry and materials science. Molecular chirality has also attracted interest in basic scientific research in fields such as molecular recognition, asymmetric synthesis, and molecular optical devices. Determination of the absolute configuration and enantiopurity is critically important in drug production and material sciences, prompting scientists to develop a variety of detection techniques [1–3]. Among the chiral detection technologies, supramolecular sensors based on molecular complexation have made significant progress in recent years. Complexation of a chiral/achiral host molecule with a chiral guest molecule through non-covalent interactions including hydrogen bonds, van der Waals forces,  $\pi$ – $\pi$  interaction, and electrostatic interactions will lead to new supramolecular enantiomers or diastereomers that could be discriminated by corresponding spectral analysis, including chiroptical techniques (e.g., circular dichroism (CD), vibrational circular dichroism (VCD), and circularly polarized luminescence (CPL)) and non-chiral spectral techniques (e.g., NMR, UV-vis absorption, and emission spectra). Supramolecular chiroptical sensors provide a sensitive and fast-responding tool for determining the absolute configuration and enantiomeric excess (ee) of chemical compounds, which is promising for the use of real-time and high-throughput detection. Combined with the array analysis of multiple host molecules and data analysis, supramolecular chiroptical sensors could be highly promising not only for determining the absolute configuration but also for differentiating compounds of different chemical structures [4–6].

An ideal supramolecular chiroptical sensor demands the following characteristics: (1) It can strongly interact with chiral analytes so as to detect the analytes of low concentrations; (2) the supramolecular complexation can induce strong spectral responses and

differentiate a pair of enantiomers with high sensitivity; (3) the supramolecular chirality induction is real-time and can be measured directly without after-treatment; (4) the supramolecular host is easier to synthesize and chemically modify.

Prompted by the fast development of supramolecular chemistry and dynamic stereochemistry of chiral compounds, there have been a great number of reports on supramolecular sensing technology in the determination of the absolute configuration and ee values of chiral amines, carboxylic acids, amino alcohols, and other chiral compounds. A variety of supramolecular sensors have been explored, and there are several reviews on the aspect of supramolecular chiral sensors [4,5]. Macrocyclic molecules have unique sensing properties over traditional sensors, primarily due to their inherent complexing ability with well-confined cavities/binding sites. The existence of multiple binding functional groups could result in a strong and specific binding/recognition towards certain guest molecules. Many outstanding chirality sensing studies have recently emerged with chiral or achiral macrocyclic compounds. In this review, we focus on the progress of research on supramolecular macrocyclic chiral sensors in the past decade. We mainly summarize the chiral sensing with macrocyclic molecules, including chiral induction of dynamic racemic achiral compounds and chiral recognition of intrinsic chiral compounds.

The research on supramolecular chiroptical sensors can be roughly divided into two categories (Scheme 1): (1) Achiral macrocyclic sensors, which consist mainly of a chiral subunit, and their possible enantiomeric conformers that can rapidly interconvert. The complexation with a chiral guest molecule will retard/inhibit the conformational interconversion and lead to conformers with diastereo- or enantio-preference. (2) Chiral macrocyclic sensors, which can form a diastereomeric complex with chiral guests. In this case, a pair of enantiomers can be differentiated by the difference of the binding affinities between the host and the enantiomers. Additionally, the diastereomeric complexes formed by the host and enantiomeric guests can have different properties so as to provide different spectral signals in, for example, UV-vis, fluorescence, and other spectra [5,6].



**Scheme 1.** Sensing mechanisms for (a) achiral macrocyclic molecules and (b) chiral macrocyclic molecules.

## 2. Achiral Macroyclic Host

For an achiral host molecule, the complexation affinity should be the same toward a pair of enantiomeric guests, and the host molecule should not be able to differentiate the

pair of enantiomers by commonly used spectroscopic methods, such as UV-vis, fluorescence, and NMR spectroscopies. Chirality sensing through complexation with an achiral host has to be accomplished by means of chiroptical technologies, such as electronic CD, VCD, or CPL [7,8]. The complexation with a chiral guest will induce conformational changes of the achiral macrocyclic host, and a pair of enantiomeric guests will lead to a pair of enantiomeric complexes that should be the same in terms of most of their physical and spectral properties. The electronic CD spectrum is the most extensively employed due to the high sensitivity of CD to the conformational variation of hosts/chromophores. This is particularly evident with host molecules consisting of the same chromophores where exciton coupling CD is highly sensitive to the variation of the inter-chromophore distance and angle of transitions and can provide a strong CD spectral response [9]. Another possible way to accomplish chirality sensing with an achiral host molecule is to introduce a chiral guest, which co-include with the chiral analyte to generate differentiation in the binding affinity and spectral response.

### 2.1. Chirality Sensing with Cucurbit[n]urils

Cucurbit[n]uril (CBs) is named for its shape similar to that of gourds or pumpkins (Cucurbitaceae). Hole-like compounds consist of  $2n$  methylene linked to a ring of  $n$  glycoluril having polycarbonyl groups at both ends of openings. The two ends of the macrocyclic compounds have the same size, and the cavity diameter is larger than the port diameter. The carbonyl group located at each port is equal to the number of monomers (degree of polymerization), while cucurbiturils with different degrees of polymerization have different cavity sizes and port diameters. Because of their unique rigid cavity and synergetic interaction provided by the C=O at the openings, CBs can have strong binding constants with a variety of electro-withdrawing/cationic guests. The pumpkin-like cavity can not only provide strong binding force but also significantly restrict the conformations of the guest. Chiral sensing based on the complexation with CBs has been attempted recently. However, CB[n]s is not directly available for chirality sensing as it is achiral and lacks a reporting chromophore [10–12]. Nau and co-workers [12] realized CB-based chiral recognition by forming a ternary complex of CB[8] with a dye and a chiral guest molecule and applied CD measurement for the chiral detection (Figure 1). Mixing CB[8], a dye acceptor and the chiral analyte leads to the formation of a chiral host-dye-analyte complex. The chiral aromatic analyte contained in the cavity of CB[8]s can effectively transfer chiral information to the absorption band of the co-included dye, which produces strong ICD signals and allows for chiral sensing at low analytical concentrations down to micromolar. Such a supramolecular chirality sensing system is suitable for real-time detection of chiral molecules containing an aromatic group, and for a wide range of analytes, from simple chiral organic compounds to complexed peptide sequences.

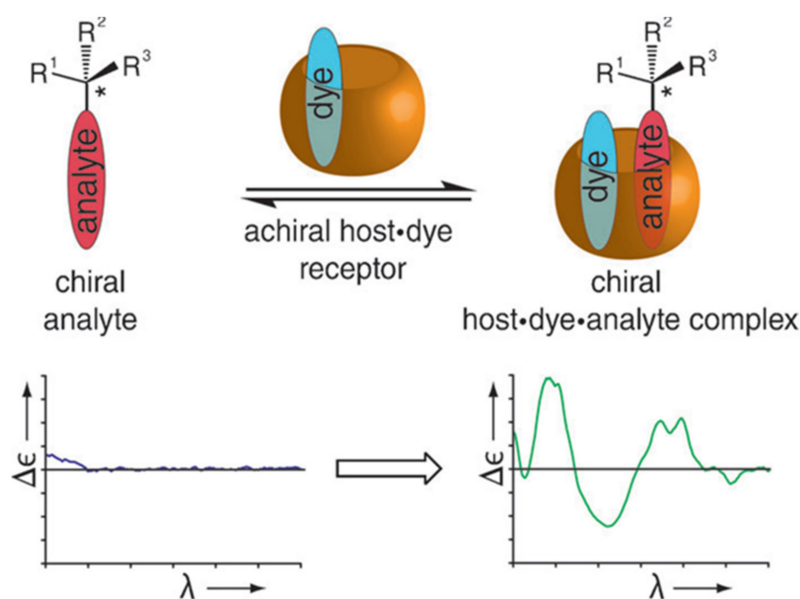


**Figure 1.** The binding process of chiral analyte with host-dye complex to form ternary complex. The weak CD signal in the far-UV region (280 nm) turns into a strong CD signal in the near-UV region (250–550 nm). Reprinted (adapted) with permission from Ref. [12] Copyright 2014 from Wiley-VCH.

However, such a CB[8]-based ternary chiral sensing system is suitable only for chiral compounds having an aromatic group that could fit into the narrow rest space of the CB[8]-chromophore complex and form interaction with the chromophore prearranged in the CB[8] cavity. Therefore, the application of this strategy for chiral alkyl compounds is restricted, and it is often difficult to achieve a strong chiroptical response for chiral alkyl compounds.

Biedermann and co-workers [7] reported a series of acyclic CB[n]s bearing aromatic side walls, which take a pre-organized C-shaped conformation. These CB[n]s retain basic binding properties while having better optical properties than macrocyclic CB[n]s. The authors synthesized acyclic CB[n]s **1** and **2**, which contain two and four anions, respectively (Figure 2). The introduction of the chromophore sidewalls allows for enhancement of the binding affinities towards organic guests due to the increased hydrophobic interactions. The complexation of **1** and **2** with chiral guests led to CD signals at the transition bands of the naphthalene moieties. For example, when the chiral aromatic amino acid *L*-Phe was added into the aqueous solution of host **1**, a strong positive CD band at 292 nm and a weak positive CD band at 326 nm were observed. The maximum CD signal induced by host **1** reached 24.18 mdeg (*D*-Trp-OMe). The enantiomer *D*-Phe gave the expected mirror-imaged CD spectra. In addition, these host molecules can be used for chiral sensing of UV-vis transparent hydrocarbon or steroids based on the hydrophobic complexation. The chiral guest-induced CD signals produced by acyclic CB[n]s **1** and **2** and cyclic CB8-MDPP are obviously discriminative and differ in their generating mechanisms. The chirality sensing with acyclic CB[n]s-chiral guest complexes is based on exciton coupling interaction, while CB8-MDPP chirality sensing is based on ICD response. Thus, the chiral supramolecular host-guest complex formed by self-assembly of achiral chromogenic host and chiral small molecule guest could provide an information-rich CD spectrum in the water medium, which has potentially broad application value in chirality sensing.

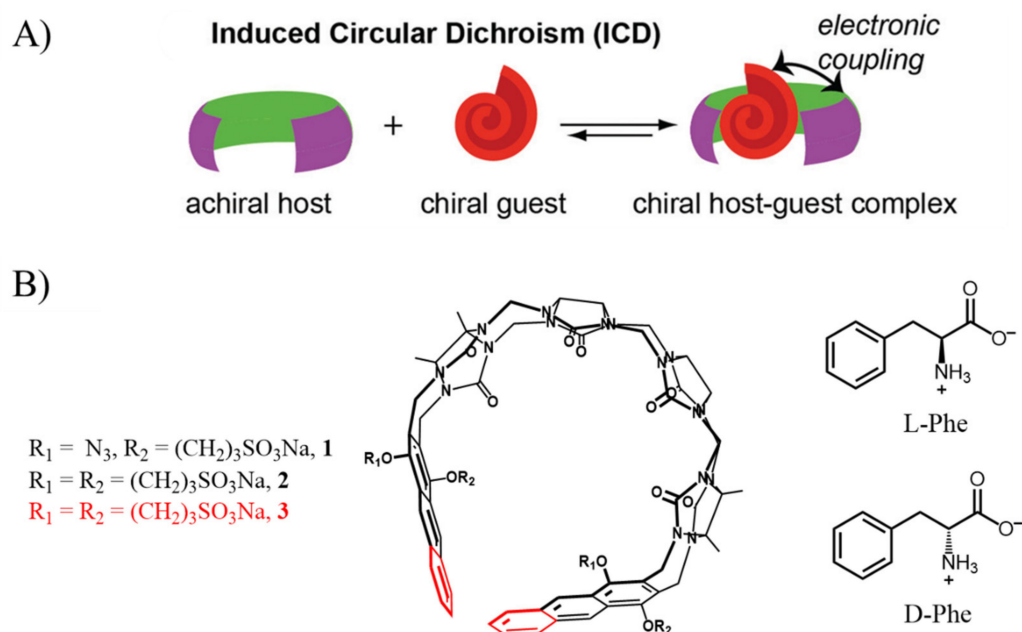


**Figure 2.** (A) The combination of subject and object of open-loop CB[n]s. Reprinted (adapted) with permission from Ref. [7] Copyright 2020 from The Royal Society of Chemistry. (B) Chemical structure of acyclic CB[n]s (**1**, **2**, and **3**) and the chiral guests L/D-Phe.

Wolf and co-workers [13] extended the naphthalene wall of acyclic CB[n]s to the anthracene wall, which takes helical structures that rapidly interconvert due to the spatial interaction between the two anthracene moieties. The chiral sensing properties of acyclic naphthalene-CB[n]s **2** and anthracene-CB[n]s **3** were further compared. Host **3** showed red-shifted UV-vis signals with increased molar absorption efficiency and a stronger CD signal (up to 50 mdeg) than host **2** for most guests. A 1:1 host-guest binding pattern was demonstrated for the complexation of host **3**. The  $^1H$  NMR studies indicated that the central hydrophobic part of the guest was located in the cavity of the host, while the cation and polar functional groups were located at the C=O portals. These acyclic CB[n]s could be used for chirality sensing of a wide range of chiral compounds, including chiral ammonium salts, alcohols, and amino acids. The produced CD signals could be conveniently used to determine the absolute configuration and enantiomeric composition of chiral guests in aqueous solution. In addition, the proportion of enantiomers could be quantitatively analyzed accurately within the error range of 5%.

## 2.2. Macrocyclic Naphthalene Derivatives

In recent years, an increasing number of macrocyclic molecules with different structures have emerged, among which macrocycles having flexible structures appear to have a unique advantage in chiroptical sensing. Jiang and co-workers [14] have, for the first time, reported the molecular recognition and chirality sensing of epoxides in water by a pair of *endo*-functionalized macrocycles composed of naphthalene subunits (Figure 3). The host molecules are highly soluble in water, and hydrophobic interaction functions as the main driving force, while the hydrogen bonds provided by the amide groups assist effective chiral transfer in the cavity of naphthalene tubes. The hydrophobic chiral epoxides, which are hydrogen bond receptors, showed good binding affinities with these naphthalene tubes, and chirality sensing of several chiral epoxides with the naphthalene tube **4** was examined in aqueous solutions. The chiral epoxides themselves have no CD response in the wavelength region longer than 250 nm. However, the chirality of epoxides was transferred to the naphthalene tube to induce a CD signal (255 nm) upon formation of the host-guest complex. The *R* configuration of several epoxides induced positive CD signals for **4**, and the *R* and *S* configurations showed a mirror image relationship. The complexes of alkyl

epoxides and aromatic epoxides with **5** showed different CD signals and even reversed CD signals, which could be used to distinguish the aliphatic and aromatic groups of epoxides. The CD signals were proportional to the enantiomeric ratios of the chiral compounds, and enantiomeric excesses (ee) values could be determined by standard linear curves fitted with concentration-dependent CD signals. The absolute error of enantiomer ratio of several epoxides was less than 4.3%. The results of a stopped-flow experiment monitoring the CD signal showed that the combination equilibrium time of host and guest was quite short (30 ms). After adding 1.0 M ammonia to the complex solution, the CD signal began to decrease with time because the inclusion constant of ammonia was greater than **R-G11**. These results allow for real-time monitoring of the production or consumption of chiral epoxides. A series of compounds containing 30 different functional groups, such as alcohol, amine, ester, ether, and flutamide, were selected for chiral induction of **4** and **5** to further explore the range of chiral sensing substrates of the naphthalene tubes [8]. The results showed that all of these chiral guests produced CD signals of chirality amplification. A few chiral compounds only induced CD signals for **4**, and the maximum induced signal intensity of **4** reached 67 mdeg, compared to a maximum induced signal intensity of 116 mdeg for **5**, demonstrating that cis-naphthalene tube has better chiral sensing performance. Naphthalene tubes **4** and **5** were complementary in chiroptical sensing suitable for a wide range of guests covering all 30 pairs of chiral molecules. In addition, they also showed good enantioselective sensing for some neutral molecules in water [15]. The amide linker of naphthalene tubes was replaced with a secondary amine linker, which can selectively recognize carboxylic acids in water by salt bridge and hydrophobic effect so as to be used for optical chiral sensing of circular dichroism-based carboxylic acids [16]. More importantly, this type of naphthalene tube is recyclable with a yield of ca. 90%.

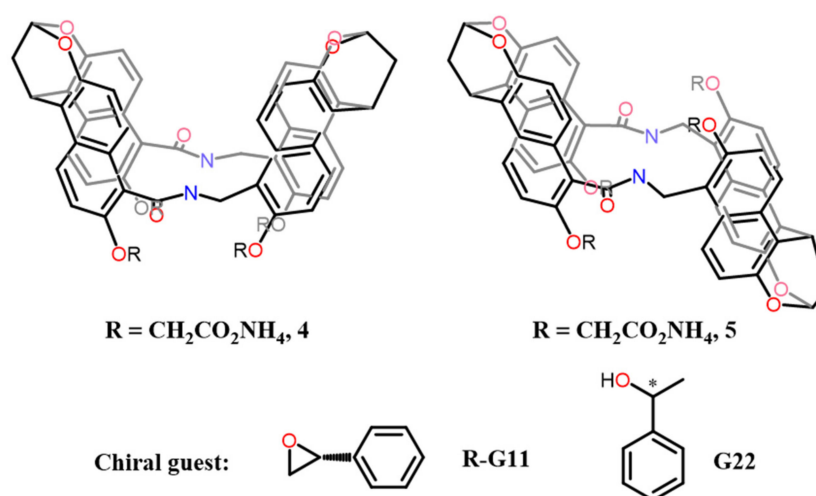


**Figure 3.** Chemical structure of the chiral guest and naphthalene tubes **4** and **5**.

The CD spectra of **4** induced by all chiral guests showed an alternating positive and negative cotton effect in the range of 230–270 nm, which might be the conformational deformation caused by the combination of chiral host and guest. The most stable binding conformation of **4** with **R-G22** and **S-G22** was calculated by DFT. It was confirmed that the acetal bridge in the two naphthalene of **4** was twisted to form a chiral conformation. In the case of **R-G22**, observed from the top of the host, the structural deformation of **4** was clockwise torsion, while **S-G22** caused a counterclockwise rotation of **4**. The structure of the two complexes was mirror image symmetric, and the degree of torsion determined the intensity of the CD signal. Hydrogen bond and C/N-H . . .  $\pi$  interactions were the torsion driving force of naphthalene tubes. When the chiral region of the guest entered into the cavity, it would cause a certain degree of torsion to produce strong CD signals, which is also the reason for the wide range of chiral sensing of naphthalene tubes. In addition, there were specific CD signals of different chiral guests in the wavelength range of 270–370 nm,

which may be caused by transition dipole coupling between the naphthalene wall and the chiral guest. However, these signals were quite small, suggesting that it was still the conformational deformation mechanism that played a dominant role in the induction of CD signals [8].

Kondo et al. reported [17] the synthesis of a bisurea-based macrocycle **6** and an acyclic bisurea analog for the purpose of chirality sensing of chiral carboxylic acid anions (Figure 4). These bisureas form a 1:1 complex with chiral carboxylates through hydrogen-bonding interaction in MeCN with high binding affinity up to  $10^7 \text{ M}^{-1}$ . Compared to acyclic bisurea derivatives, the CD signal (285 nm, 323 nm, and 350 nm) induced by carboxylic acid anions to **6** was up to 10-fold because of the rigid properties of the macrocyclic structure. On account of the hydrogen bonding between the methyl proton of the side chain of carboxylic acid and the cyclic bisureas, the increase in the side chain was beneficial for the binding affinity, and therefore the induced CD signals correlated directly to the length of the side chain of carboxylate.

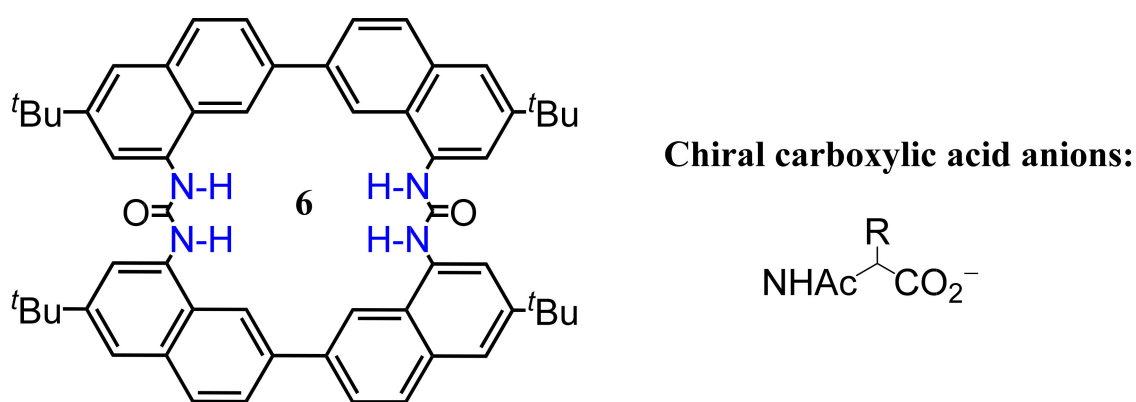


**Figure 4.** Chemical structure of the chiral guest and naphthalene macrocycle **6**.

### 2.3. Pillar[n]arenes

Pillar[n]arene derivatives have unique macrocyclic structure and excellent host-guest complexation properties [18]. Pillar[n]arene derivatives, in the absence of any chiral center, have a pair of  $R_P$  and  $S_P$  configurations that can generally rapidly rotate through the “oxygen-through-the-annulus” flipping mechanism [19–26]. By introducing a bulky guest molecule on the rim of a pillar[n]arene or interlocking an axle into the cavity to inhibit the flipping of subunit, one enantiomeric planar chirality will be preferred to generate CD signals. In the absence of a chiral guest, the two enantiomeric conformers of pillar[n]arene should have an identical population in the bulk solution. However, the chiral conformers should bind a chiral guest with unequal binding affinities, and one of the enantiomeric conformers should be more populated to induce chiroptical signals at the absorption band of pillar[n]arene. Yang and co-workers [27] reported the first pillar[n]arene-based chiral sensing by using pillar[5]arene derivatives **7–15**, which have different alkyl chain lengths. They demonstrated that the complexation of pillar[5]arene with amino acid derivatives induced strong CD responses at the absorption band of pillar[5]arene (Figure 5). The  $\alpha$ -amino acid ethyl ester salts showed strong binding affinities (association constants  $> 10^5 \text{ M}^{-1}$ ) with pillar[5]arenes, and induced CD signals with the maximum CD signals at around 310 nm. Increasing the concentration of  $\alpha$ -amino acid derivatives in pillar[5]arenes solution, the fluorescence emission of hosts was continuously enhanced due to the complexation-fixed framework. The complexation of *L*-amino acid derivatives showed a perfect mirror symmetry relationship to the complexation of *D*-amino acid, and the CD intensities appeared proportional to the enantiomeric ratio, manifesting an ideal chiral sensing of the absolute configuration enantiomeric purity of chiral amines with an average error of 2.2%. In addition, the same amino acid could induce CD signals that

differed significantly with pillar[5]arene derivatives having different alkyl chain lengths, even leading to an inversion of CD signals. The complexation of pillar[5]arene derivatives and amino acids showed a good entropy-enthalpy compensation relationship, indicating that the main driving force of complexation did not change with the chain length of the pillar[5]arene alkyl ether. The diversity of CD responses and the dependence of different chiral amines on the length of pillar[5]arene alkyl chains provide a powerful host library for differentiating not only the absolute configuration but also different  $\alpha$ -amino acids.

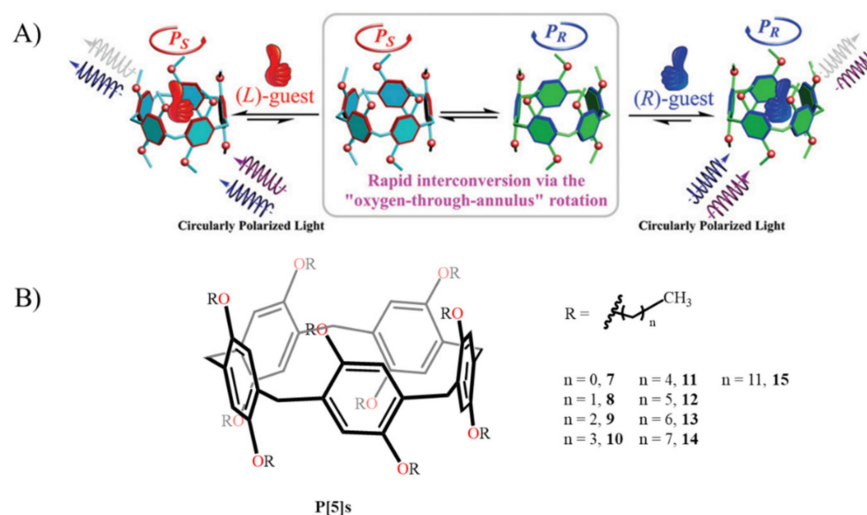


**Figure 5.** (A) Mechanism of planar chiral induction of P[5]s. Reprinted (adapted) with permission from Ref. [27] Copyright 2020 from The Royal Society of Chemistry. (B) Chemical structures of P[5]s with different chain lengths.

Huang and co-workers [28] synthesized water-soluble pillar[n]arenes (**16** and **17**) in order to determine the chirality of chiral molecules in water (Figure 6). When the water-soluble pillar[n]arene derivative **16** respectively complexed a pair of enantiomeric amino acids in water, mirror-imaged CD spectra were observed. When the host-guest binding was decreased by increasing temperature, the induced CD signal was significantly reduced. The addition of the same amino acid to **17** induced a CD signal opposite to that with **16**, exhibiting an odd-even effect of the repeating number of the hydroquinone ether rings. In addition, when chiral guests propylene oxide and 3-butyn-2-ol were mixed with **16** or **17**, respectively, only **17** successfully induced a CD signal, which was ascribed to the different host-guest binding strength; the stronger the binding strength, the more intense the induced CD signals. The DFT calculation suggested that the  $Rp$ -7- $L$ -Arg complex was more stable than  $Sp$ -7- $L$ -Arg, which was consistent with the fact that  $L$ -Arg induced a positive CD signal. Such differentiation is due to the chiral match/mismatch effect of the diastereomeric host-guest complex. Compared to other macrocycles, such as  $\beta$ -cyclodextrin, cucurbit[6]uril (CB[6]), carboxyl-bearing water-soluble cyclotrimeratrylene (CTV), and  $p$ -sulfonatocalix[4]arene (SC4A), the pillar[n]arenes, have inherent advantages and unique characteristics, including high affinity, detectable UV-vis absorption, and inducible chirality in chiroptical amplification.

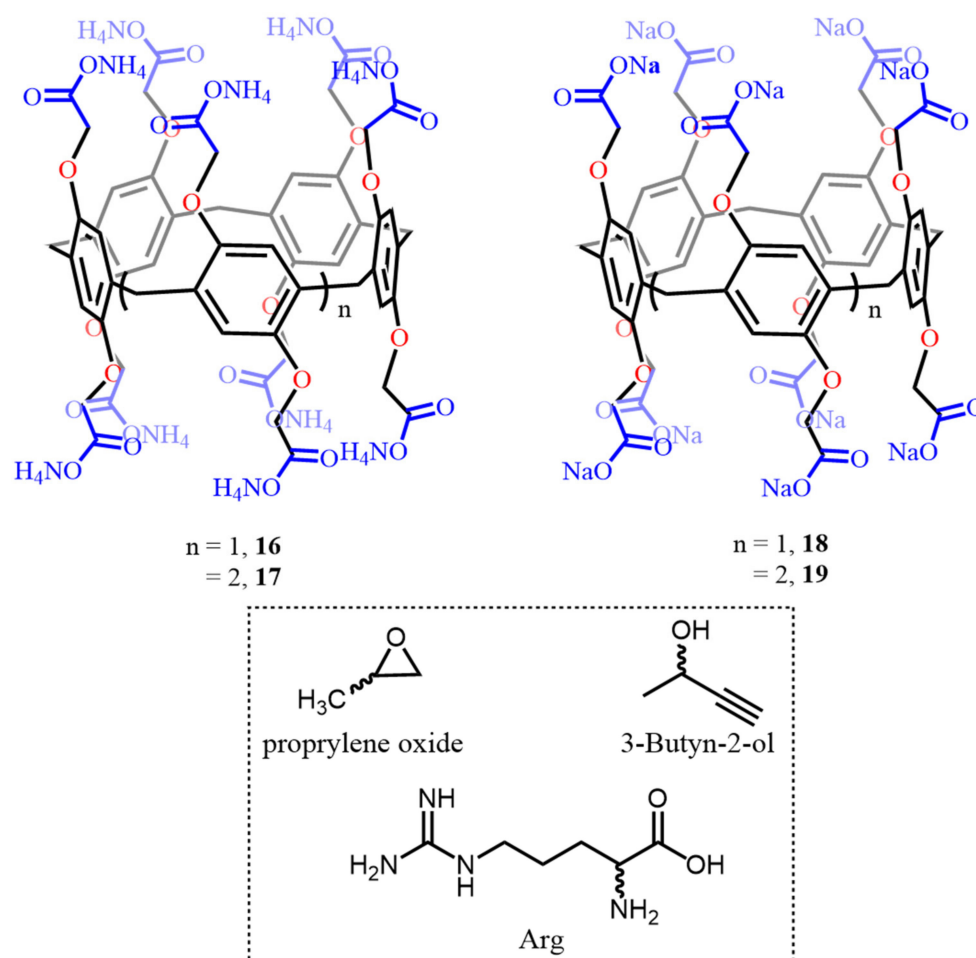


**Figure 6.** Chemical structures of water-soluble P[n]s with different cationic and their chiral guests.

Similarly, Wang group [29] synthesized a water-soluble pillar[n]arene **18** and studied its chiroptical induction with 19 different *L*-amino acid ethyl ester hydrochlorides. Among the guests, *L*-Arg-OEt induced the opposite configuration of **18** compared with the other *L*-amino acid ethyl ester hydrochlorides, which was attributed to the different binding of the chiral parts of amino acids, such as the side chain part or the ethyl part, to the cavity of **18**. Inspired by these results, a sensor capable of recognizing different chiral regions of a single amino acid derivative was studied [30] by using **18** and its homolog **19** (Figure 6) as the supramolecular sensors. Cotton CD signal at 303 nm of **19** induced by *L*-Phe-OEt and *L*-Arg-OEt hydrochlorides was reversed compared to **18**. The 2D NOESY analyses for the complexation of *L*-Phe-OEt or *L*-Arg-OEt with **18** or **19** demonstrated that the binding region was the ethyl ester group or the  $\alpha$ -side chain, respectively. The complexation of *L*-Phe-OEt or *L*-Arg-OEt and **18** or **19** was simulated by DFT calculation, which was consistent with the experimental results, elucidating that the major driving forces for chiral differentiation includes hydrogen bonding, C/N-H... $\pi$  interactions,  $\pi$ - $\pi$  stacking, etc. The binding affinity between **19** ( $7.74 \times 10^{-4} \text{ M}^{-1}$ ) and *L*-Arg-OEt was slightly lower than that of **18** ( $8.54 \times 10^{-4} \text{ M}^{-1}$ ). The 1:1 mixture of **18** and *L*-Arg-OEt gave a negative CD signal that peaked at ca. 300 nm. However, adding 0.2 eq **19** led to an inversion of the CD signal, and the positive CD peak gradually increased with increasing concentrations of **19** in the complex of *L*-Phe-OEt and **18**, demonstrating a shift of complexation.

Ogoshi and co-workers [31] established a ternary chiral sensing system using a carboxylated pillar[5]arene as the receptor, 1-cyclohexylethyl amine as a chiral inducer, and 1,4-dibromobutane as a regulatory factor, and applied the pillar[5]arene derivative to chirality memory. It was demonstrated that the order of addition of the chiral inducer and the

regulatory factor could critically affect the chiral induced signals of the chiral receptor. The induced planar chiral signals could be controlled and memorized by heating and cooling the ternary system.

#### 2.4. Cyclic Octapyrroles

Chiral biomacromolecules such as DNA play essential roles in the storage and encoding of genetic information. However, the CD signals of most biomacromolecules are not strong, or the absorption band of chromophores is shorter than 200 nm, which presents a challenging task to identify and detect the conformational properties of these macromolecules and gain insight into their functional mechanisms. In this regard, the supramolecule chirality transfer strategy provides a promising tool for chiral sensing of biological macromolecules. Cyclic oligopyrrole and its metal complexes take a helical conformation, and the pair of enantiomeric conformers can dynamically interconvert at room temperature. In 2009, Setsune et al. [32] successfully induced helical preference by adding mandelic acid or 1-(1-phenyl) ethylamine to the complex of cyclic octapyrrole and the metal Cu. However, the cyclic host acquires induced chirality through multiple interactions with the small chiral molecule in its inner cavity or metal center, and there is no application of cyclic octapyrrole as a chiral sensor for macromolecules.

Tsuda and co-workers have used the cup-shaped octapyrrole for chirality sensing of oligonucleotides [33]. By electrostatic and/or hydrophobic interaction, when the same amount of nucleotide monomer dAMP, dTMP, dCMP or dGMP was respectively complexed with **20** (Figure 7) in a pH 4.0 acetate buffer solution, the UV-vis absorption peak  $\lambda_{\max}$  of **20** slightly blue-shifted from 543 nm to 542 nm, and the absorbance increased while no CD signal was induced. When **20** was mixed with a homooligonucleotide, the spectral changes demonstrated that homooligonucleotide formed a complex with **20** by non-covalent interaction, which is essentially different from nucleotide monomer. However, induced CD spectra only appeared with dA<sub>12</sub> and dT<sub>12</sub>. The mixture of **20** and dA<sub>12</sub> showed negative CD signals at 787 and 477 nm, and positive CD signals at 617 and 405 nm, respectively, indicating that an *M, M* helical conformation was induced for **20**. Under the same conditions, the CD spectra of the mixture of **20** and dT<sub>12</sub> were primarily the same as those of **20** and dA<sub>12</sub>. The experimental results showed that **20** has a 1:1 complex relationship with dA<sub>12</sub>, and formed a 1:1 complex and a 1:2 complex with dT<sub>12</sub> successively (Figure 7). dT<sub>12</sub> encapsulates **20** in an aqueous solution by hydrophobic interaction. Here, a thymine component of dT<sub>12</sub> containing a hydrophobic methyl group but no amino group could conduct supramolecular complexation with **20** to induce a spiral structure. The CD signal changed with the content of thymine in dT<sub>n</sub>A<sub>12-n</sub>. Therefore, **20** can sense the molecular chirality of homooligonucleotide having a high content of thymine, which provides a good prospect for the chiral sensing of DNA or protein and other larger molecules.

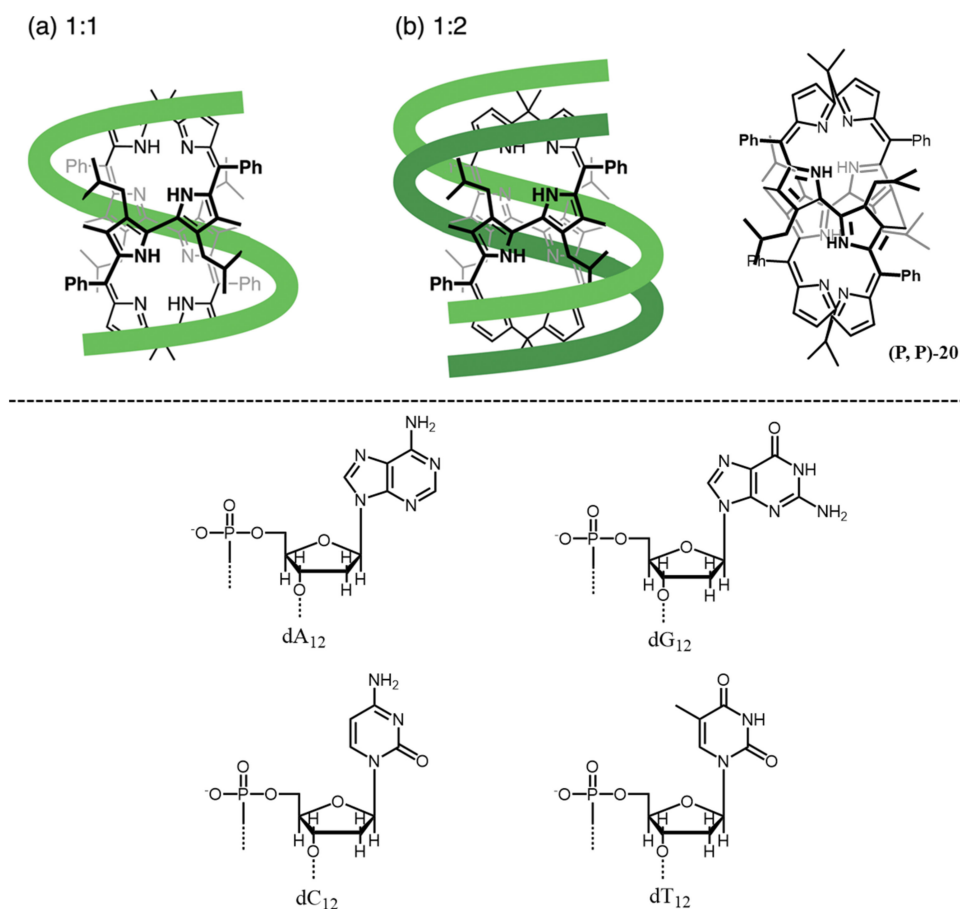


**Figure 7.** Possible associations of **20** turning to (*M, M*)- conformation and dT12 in (a) 1: 1 and (b) 1: 2 complexations. Reprinted (adapted) with permission from Ref. [33] Copyright 2020 from The Royal Society of Chemistry. Additionally, the chemical structure of (*P, P*)- conformation of **20**. Chemical structure of nucleotides and oligonucleotides.

### 2.5. TPE-Based Macrocycle

Achiral tetraphenylethene (TPE)-based macrocyclic molecules comprise a pair of racemic conformers with both left-handed and right-handed chirality. TPE molecules with propeller-like *P/M* rotating conformation and AIE properties are ideal cornerstones for exploring dynamic conformational chirality during chiral transfer. For example, Zheng and co-workers [34] synthesized a class of novel tetrastylene triangular macrocycles with tri-crown ether rings using ethylene bridges, which showed aggregation-induced emission (AIE). Due to the interaction between chiral acids and crown ether ring protons, strong CD and CPL signals were generated in the thin films formed by this complex, which are attributed to the single-handed propeller conformation induced by the TPE unit rather than the supramolecular spiral fiber self-assembled structure.

Cao and co-workers [35] synthesized two macrocyclic **21** and **22** with different TPE groups (Figure 8A). When a series of negatively charged nucleotides (AMP, ADP, ATP, UTP, CTP, and GTP) were added as guest molecules into the solution of **21** and **22**, the fluorescence intensity of the two large macrocycles increased to a certain extent, respectively. It was demonstrated that these macrocycles could encapsulate two nucleotide molecules in a hydrophobic cavity to form a 1:2 inclusion complex. The chiral center of the complexed guest molecule was far from the TPE group, with the nucleotides entering into the cavity, and therefore, no obvious CD signal was induced. When smDNA or ctDNA was added to the solution of **21**, a negative CD signal appeared in the 300–450 nm region, corresponding to the *P* helix conformation of the macrocycle. In addition, the positive and negative CD signals in the range of 200–270 nm and 270–320 nm were due to the binding of the TPE

unit of **21** to the groove of the DNA, resulting in the *P* conformation of **21**. Due to the steric hindrance of anthracene groups, **21** could not enter the grooves of DNA well and led to only a weakly induced CD signal (Figure 8B). TPE fluorescence was enhanced due to inhibition of free rotation by grooves of DNA, suggesting that **21** could be used as a fluorescent switch for DNA detection. These macrocyclic molecules could thus recognize biomolecules, such as nucleotides and DNA, through multiple orthogonal responses, which improves the accuracy of detection and identification of biomolecules in biocompatible media.

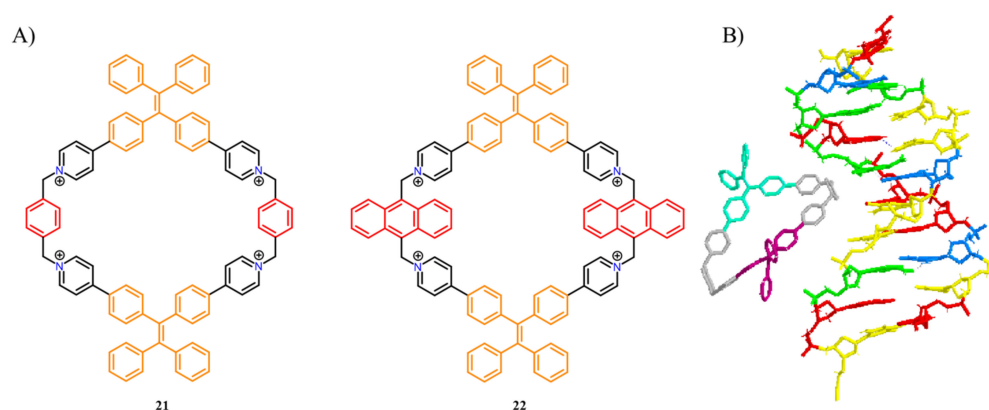


**Figure 8.** (A) The chemical structure of **21** and **22**. (B) The possible complex structure of **21** with DNA.

TPE units have been introduced into an octa-cationic cage to give a meso-racemic compound because the two TPE cells in the cage adopt *P* and *M* helical conformations simultaneously [36]. Because of the existence of eight electron-defective pyridine rings, cage **22** was able to recognize electron-rich guest molecules well through C-H... $\pi$  interaction and electrostatic interactions in water (Figure 9). The NMR studies indicated that 5'-adenosine monophosphate (**A**) enters the cavity of the cage completely, and its adenine unit locates in the center of the cage with the monophosphate group positions at the edge part of the cage. The host-guest complexation ratio was demonstrated to be 1:2. The deoxynucleotides cannot form stable base pairs in water due to interference from strong hydrogen bonds with water molecules, and the hydrophobic cavity of the cage is conducive to the formation of the hydrogen bond base-pair **A**<sub>2</sub> in **22**⊃**A**<sub>2</sub> complex. When deoxynucleotide was added to the aqueous solution of **22**, a strong CD signal appeared at 300–450 nm, suggesting that host-guest complexation favors the host conformation with a kinetically stable co-rotation. The negative CD signal in the 300–450 nm region indicated that the chiral guest promoted the conversion of **22** towards *P*, *P* conformation, while there were two stronger negative and positive CD signals at 200–250 nm and 250–300 nm, which were assigned to the  $n\text{-}\pi^*$  and  $\pi\text{-}\pi^*$  transitions of **22** and **A**, respectively. This result suggests that the chiral transfer and induction are due to the free conformational interconversion limitation and the improved population of the chiral conformation caused by the complexation between the cage and the guest. The guest molecules **T** and **C** also showed a similar chiral induction behavior. On the contrary, 5'-guanosine monophosphate (**G**) experienced chiral reversion upon increasing the concentration, exhibiting an obvious two-step complexation. Although part of the CD signal at the short wavelength reversed, the long wavelength kept a negative CD signal, revealing that **22**⊃**G**<sub>2</sub> complex is the *P*, *P* conformation. When complexed with **A**<sub>2</sub>, **T**<sub>2</sub>, **C**<sub>2</sub>, or **G**<sub>2</sub>, the cage exhibited the unique adaptive chirality of the *P*, *P* rotational conformation of the TPE units. Furthermore, based on the AIE properties of TPE, the complexed gels of **22** with deoxynucleotides showed strong CPL signals, which provide other opportunities for the manufacture of biocompatible CPL materials.

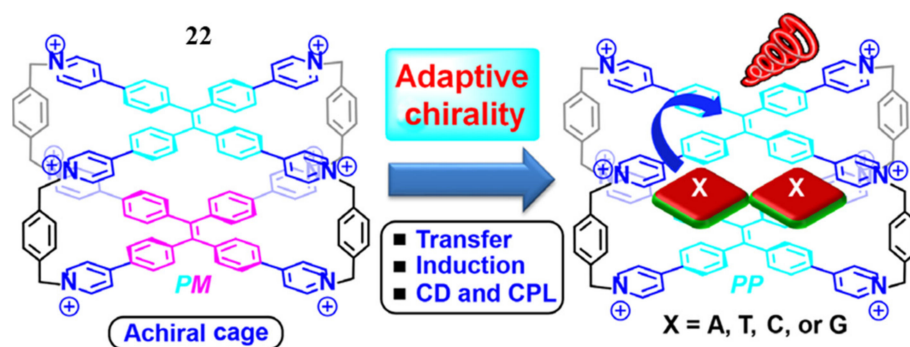


**Figure 9.** Mechanism of adaptive chirality of **22** produced by interaction with nucleotides. Reprinted (adapted) with permission from Ref. [36] Copyright 2020 from CCS Chemistry.

## 2.6. Other Macrocycles

More and more new macrocyclic molecules have been employed as host molecules for chirality sensing through conformational chirality transformation. The perylene diimide (PBI) macrocycle **23** (Figure 10) exists in solution as a mixture of racemates composed of (*M, M*), (*P, P*), and (*M, P*)/(*P, M*) stereoisomers. Chiral guests (*S*)-**G2**, (*S*)-**G3**, and (*S*)-**G4** induced the conformational chirality of the host molecules by preferring one of the chiral conformers of the PBI macrocycle, resulting in a shift in the conformational equilibrium between the stereoisomers [37]. The binding of the guest molecule (*S*)-**G4** to the host PBI macrocycle has been studied by  $^1\text{H}$  NMR techniques. The results of  $^1\text{H}$  NMR titration and  $^1\text{H}$ - $^1\text{H}$  COSEY showed that the proton peaks of free guest decreased and the split signal peak of host-guest complex increased upon the addition of (*S*)-**G4**. The complexation kinetics were investigated by time-dependent  $^1\text{H}$  NMR, which demonstrated a quasi-first order, and the rate constant  $k_{obs}$  was determined by calculating the slope of the linear part of the corresponding natural logarithmic graph. The  $k_{obs}$  showed positive correlation with the concentration (2–10 eq.) of (*S*)-**G4**. The rate constants of isomerization of host  $k_{iso}$  and guest  $k_{ex}$  were roughly estimated based on the temperature-dependent  $^1\text{H}$  NMR experiments of the host with and without (*S*)-**G4**, respectively, in  $\text{CDCl}_3$ .

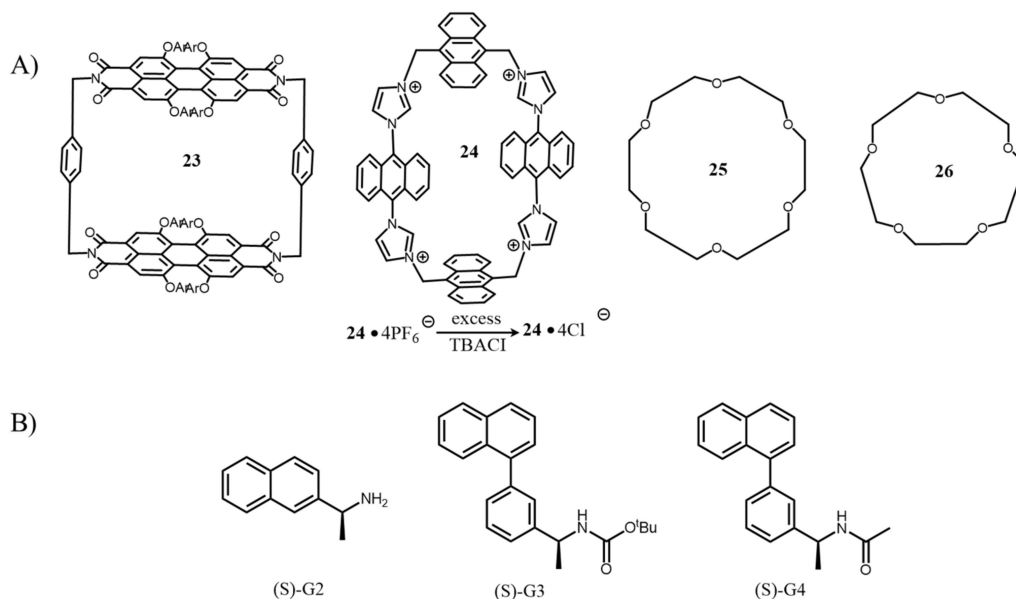


**Figure 10.** (A) Chemical structure of **23**, **24**, **25**, and **26**. (B) Chemical structure of chiral guests.

Cao et al. [38] synthesized an anthracene-based four-ion host **24** (Figure 10), which has good solubility in water. ITC titration revealed that the complexation ratio of **24** to nucleotides (ATP, GTP, CTP, and UTP) was 1:1. All the four nucleotides could complex

with **24** to generate CD response, and the CD signal induced by GTP and ATP was opposite to that of the other two nucleotides. The competitive complexation of GTP and UTP led to inversion of CD signal. The tricenter hydrogen bond dominates the complexation between **24** and nucleotides to induce the *M*- or *P*-twisted conformation. ATP can promote the intermolecular *P*-distortion stacking of anthracene rings between **24**, and generate a strong CPL signal in water. The macrocycle can lead to hierarchical chirality, including adaptive chirality and host-guest complex-induced aggregation chirality, which provides the possibility for the identification of biomolecules with tiny differences.

The strategy of the complexation-induced conformational variation for chiral sensing could be sensitively detected by CD or CPL spectra. In addition, some non-chiral supramolecular macrocycles, such as crown ethers **25** and **26** (Figure 10), have been used to complex chiral ammonium salt  $\alpha$ -methyl benzylammonium (MBA) chloride [39], which led to novel VCD characteristics assignable to the crown ether vibrational mode. The MBA-H<sup>+</sup>/**25** complex preferred a unichiral D3D symmetric conformation, while the crown ether of the MBA-H<sup>+</sup>/**26** complex contributed less to the VCD characteristic and was entirely due to the conformational chirality. The application of VCD to chiral sensing is still limited, but should be expanded to novel non-chiral supramolecular macrocycles, especially those with no chromophores.

In order to improve the sensing accuracy to thus precisely determine the enantiomeric ratios, it is very important to achieve intense CD signals and high *g* factor values upon chiral induction. In addition, it is preferred to broaden the range of chiral substrates. The chiral sensing parameters obtained with the achiral macrocycles are summarized in Table 1.

**Table 1.** The detection method, targeted substrates, CD signal peak wavelength ( $\lambda_{\max}$ ), maximum CD signal value ( $\Delta\theta_{\max}$ ), and binding constants ( $K_a$ ) obtained with achiral macrocyclic chiral sensors.

Achiral Macrocycle	Detection Method	Targeted Substrates	$\lambda_{\max}/\text{nm}$	$\Delta\theta_{\max}/\text{mdeg}$	$K_a/M^{-1}$
<b>1</b>	CD	hydrocarbons, terpenes, steroids, amino acids, and drugs	292 and 326	24 (D-Trp-OMe)	$10^2\sim 10^6$
<b>3</b>	CD	ammonium salts, amino acids, alcohols, and terpenes, purely aliphatic structures	270 and 380	50 (2-(1-Aminoethyl)Naphthalene)	$10^6$
<b>4 and 5</b>	CD	epoxide, alcohol, amine, ester, ether, acetal, sulfinamide, and sulfoximine	255	67 for <b>4</b> 116 for <b>5</b> (epoxides)	$10^2\sim 10^6$
<b>6</b>	CD	carboxylic acid salt	285, 323, and 350	80 (Ac-LeuO <sup>−</sup> )	$10^5\sim 10^7$
<b>7–15</b>	CD	amino acid ester BARF salt	283 and 310	40 (L-Phe-OMe)	$10^4\sim 10^5$
<b>16 and 17</b>	CD	amino acids, propylene oxide, and 3-butyn-2-ol	310 and 283	5 (Arg)	$10^4$
<b>18 and 19</b>	CD	amino acid ethyl ester hydrochlorides	303 and 247	25 for <b>18</b> (L-Ala-OEt)	$10^4$
<b>20</b>	CD	homooligonucleotide	405, 477, 617, and 787	20 (dT <sub>11</sub> )	\
<b>21</b>	CD	DNA	200~270, 270~320, and 300~450	10 (smDNA)	\
<b>23</b>	CD	naphthalene derivatives	581	38 (naphthalene derivatives)	\

### 3. Chiral Macrocyclic Host

#### 3.1. BINOL-Based Macrocycle

Binaphthols (BINOLs) are compounds that have axial chirality. A number of BINOL-based chiral fluorescence sensors have been exploited because of their unique luminescent

properties [40,41]. Recently, a variety of new BINOL-based macrocycles emerged [42–46]. Anzenbacher and Ema et al. reported [42] a class of macrocyclic hosts composed of chiral binaphthalene and hydrogen bond donors to recognize chiral carboxylic acids. Four BINOL-based macrocyclic molecules (Figure 11) were synthesized by cyclization at the 3,3'-positions of the BINOL. The macrocyclic chiral cavity could complex different analytes to regulate chiral induction, and the fluorescence of the introduced chromophores could be enhanced or quenched. The fluorescence of **29** and **30**, which have electron-rich fluorophores, was enhanced by inhibiting the energy dissipation of the excited state after the binding of anions, while fluorescence quenching was observed with **27** and **28** due to the binding of anions, while fluorescence quenching was observed with **27** and **28** due to the photoinduced electron transfer (PET). The 1:1 stoichiometric binding ability of the chemical sensor with selected carboxylate was tested by electrospray ionization (ESI) mass spectrometry. (R)- and (S)- carboxylic acids exhibited great differences in fluorescence intensity upon binding with **27**, **28**, **29**, or **30**. Linear discriminant analysis (LDA) was applied to analyze the fluorescence intensity output of the mixtures of the host and the chiral analyte at different wavelengths, which allowed for identifying enantiomers of various carboxylic acids, and enantiomers of chiral analytes could be separated with 100% accuracy. Quantitative and semiquantitative experimental results showed that the sensors **27**–**30** can accurately determine enantiomer excess in the solution with errors < 1.6%. In addition, (R)-BINOL-based macrocycles without the conjugated groups were synthesized to recognize chiral carboxylic acids [43]. By calculating the inclusion constants as a judgment of chiral recognition ability, the macrocycles' cavity size and appropriate geometry were demonstrated to play an important role in effective enantiomer recognition.

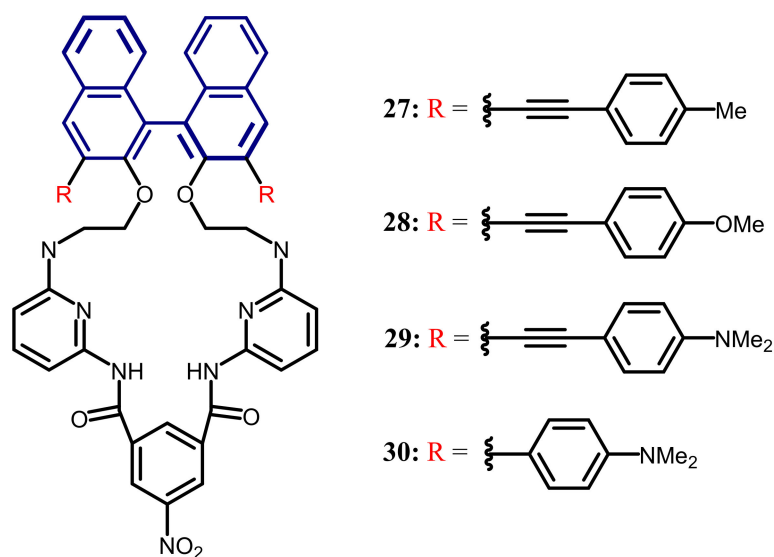


**Figure 11.** The chemical structure of **27**, **28**, **29**, and **30**.

Macrocycles containing pyridine-acetylene-phenol units have previously been verified to have a high affinity for monosaccharides and extract monosaccharides from aqueous solutions into lipophilic solvents [44]. Two macrocyclic molecules [46], (S)/(R)-**31** and (S)/(R)-**32**, which can enantio-selectively recognize monosaccharides (Figure 12), were designed by combining this unit with the BINOL. The hydroxyl groups in phenol and BINOL acted as hydrogen bond donors, and pyridine served as hydrogen bond receptor, which could lead to a push-pull system with monosaccharides (Figure 12B). The association constants of oct- $\beta$ -D/L-Glc, oct- $\beta$ -D/L-Man, oct- $\beta$ -D/L-Fru, and (S)-**31** or (S)-**32** were determined to be a 1:1 binding model. Compared with the high binding affinity and excellent enantioselectivity of (S)-**31** for octyl glycosides, the binding constant of (S)-**32** is an order of magnitude smaller and has almost no chiral recognition ability.  $^1\text{H}$  NMR studies on the binding of octyl glycosides revealed that (S)-**31** and (R)-**31** or (S)-**32** and (R)-**32** have different hydrogen bonding patterns in the chiral recognition of oct- $\beta$ -D/L-Fru.

The binding of glycosides by macrocycles was studied by solid-liquid extraction experiments. For example, after mixing D-fructose powder into a (S)-**31** DCE solution stirred for 10 h, the insoluble matter was filtered to detect the CD signal. The CD signal of (S)-**31** at 350 nm was significantly increased and red-shifted, indicating the formation of a new host-guest complex. This phenomenon also occurs in L-fructose extraction, where the CD signal shows a greater redshift than that of D-fructose. Further extraction was performed with the 1:1 racemic mixture of fructose enantiomers, and the CD signal was found to be consistent with the complex of D-fructose and (S)-**31**, which proved that (S)-**31** has a stronger affinity for D-fructose. The other three macrocycles are also capable of similar enantioselective extraction. These hosts, which can be specifically recognized and extracted from racemic mixtures, are expected to play an important role in separating mixed products in the enantiotropic reaction of sugars.

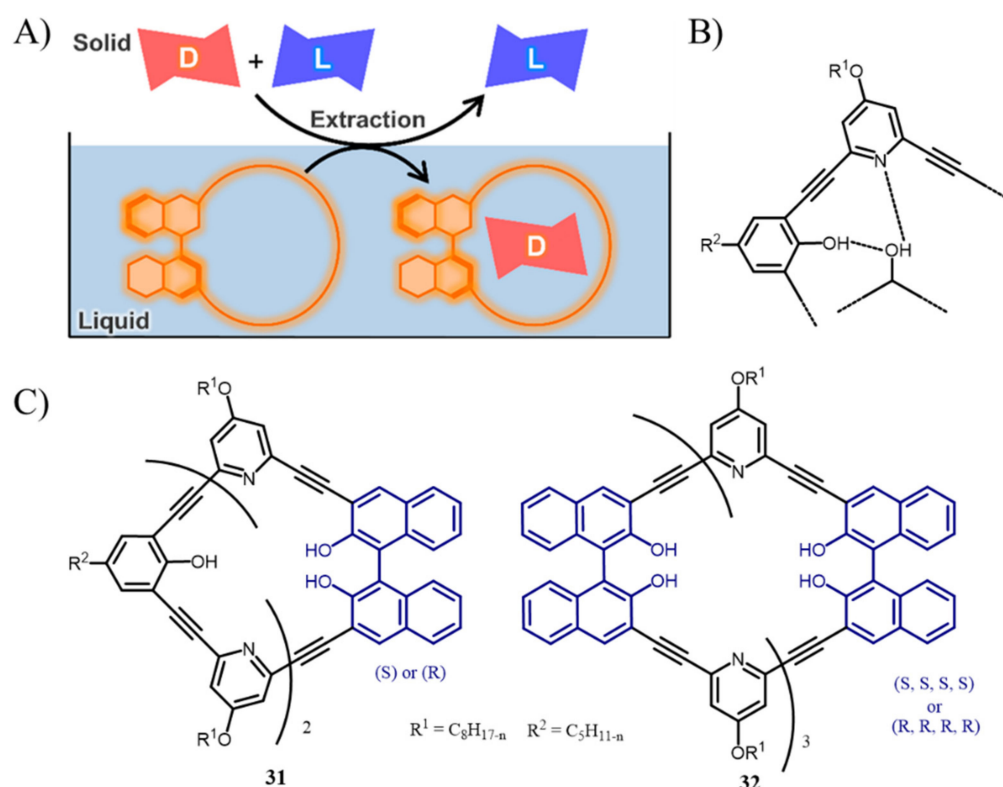


**Figure 12.** (A) Mechanism of chirality recognition of **31** and **32** for guests. Reprinted (adapted) with permission from Ref. [46] Copyright 2019 American Chemical Society. (B) The push–pull hydrogen bonding between guest and host. (C) Structure of BINOL–based macrocyclic receptors **31** and **32**.

### 3.2. Triptycene-Based Macrocycle

Triptycenes, which are rigid aromatic scaffolds that can endow macrocycles with chiral and electron-rich cavities, have been applied to the construction of macrocyclic compounds. The rigid structure of macrocycles composed of three 2,6-dihydroxytriptycene subunits bridged by methylene groups has a fixed chiral conformation and symmetrical structure [47]. The electrically rich helical chiral cavity showed high affinities for electrically deficient guest molecules and excellent chiral recognition towards chiral quaternary ammonium salts. The macrocycle rac-**33** was derivatized by reacting with *d*-(+)-camphorsulfonyl chloride in CH<sub>2</sub>Cl<sub>2</sub> and successfully diastereo-separated into 2,6-helic[6]arenes *P*-**33** and *M*-**33** (Figure 13). When rac-**G1** was added to the acetone-*d*<sub>6</sub> solution of *M*-**33**, the proton peaks of *R*-**G1** and *S*-**G1** shifted differently. Compared to the doublet peak of the proton H<sup>1R</sup>, the proton H<sup>1S</sup> showed a broadened peak first and then gradually changed into a doublet peak with the increase in host/guest ratio. The apparent difference in peak shape was due to the difference in the complex structure of the enantiomeric guests and the host,

which provides a succinct yet powerful strategy for detecting the absolute configuration of the chiral guests. In addition, the distinguishable change in the chemical shifts of proton  $H^{1S}$  and proton  $H^{1R}$  indicates that *M*-33 has a higher binding affinity for *S*-G1 so as to recognize chiral G1 enantioselectivity. *P*-33 showed an opposite preference for enantiomers of G1 with a  $K_R/K_S$  value of 4.91/1, which is in contrast to the  $K_R/K_S$  value of 1/6.67 for *M*-1. Hosts *P*-33 and *M*-33 also exhibited excellent enantiomeric recognition for bioactive carnitine and naphthylethylamine, in which *M*-33 prefers the *S* configuration while *P*-33 prefers the *R* configuration.

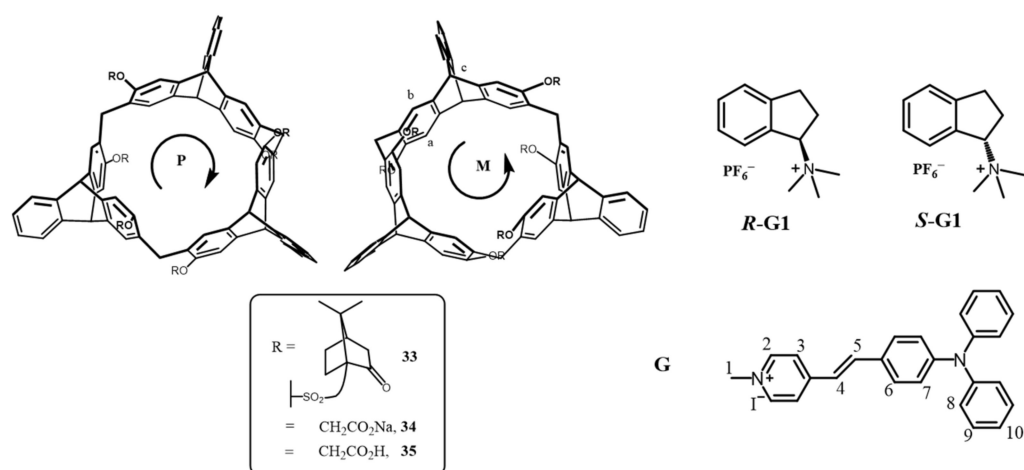


**Figure 13.** The enantiomer of 33, 34 and 35. The chemical structure of G1 and G.

Several water-soluble chiral helic[6]arenes derivatives *P*-34 and *M*-34 were synthesized by virtue of ready modification of hydroxyl groups at the 2,6-position of triptycene [48]. These macrocycles could form a 1:1 complex with 4-[(4'-N, N-diphenylamine) benzene-methyl iodopyridine] (**G**) in water. The UV-vis absorption peak of **G** at 450 nm and the fluorescence emission peak at 600 nm were bathochromic shifted to 475 nm and 618 nm, respectively, after one equivalent *P*-34 was added (Figure 13). The host-guest complexation enhanced the fluorescence, possibly due to the spatially inhibited aggregation-induced quenching (ACQ) effects of the guest. According to NMR studies, it was deduced that the pyridine part of the guest entered into the cavity, while the two benzene rings were connected by the double bond located outside the cavity.

The host-guest complexation at concentrations of 0.1 and 0.6 mM, respectively, was investigated in THF/H<sub>2</sub>O = 2:1 (*v/v*), which showed a pair of mirror-symmetric induced CD signals peaked at 425 nm and 475 nm, respectively, as the result of chirality transfer from macrocycle to the guest. The pH and temperature variations well-regulated the host-guest complexation between **G** and *P*-34, resulting in the change of CD intensity, which confirmed that the induced CD signals arose from the non-covalent host-guest interaction. In addition, the CPL signals of the complexes *P*-34·**G** and *M*-34·**G** near 620 nm were also observed and showed a temperature- and pH-dependent response.

Moreover, Chen and co-workers [49] have recently reported a chiral macrocyclic host composed of 1,4-dimethoxybenzenes and triptycenes, which exhibit enantioselective recognition of biologically active amino-saccharides. The *P*-helical host preferred *R*- guest, and the enantioselectivity ratio was as high as 3.89.

### 3.3. Bambusurils

Chiral macrocycles based on *n*-ethylene ureas have been used to bind inorganic anions, while their inherent chirality provides the possibility for enantiomer recognition of chiral anions [50,51]. Sindelar and co-workers [52] developed bambus[*n*]urils (*n* = 6) with *n*-ethylene ureas being bridged by methylene bridges, yielding two different compounds 35 and 36 (Figure 14). The binding ratio of 35 to guest *S*-G1 was determined to be 1:1 by

$^1\text{H}$  NMR spectral studies. Due to the slow exchange of free and complexed hosts on the NMR timescale, the concentration and binding constants of the two compounds could be determined by the integration of proton signals. It was demonstrated that **35** and **36** showed different binding affinities towards enantiomers of chiral carboxylic acids. For example, **35** binds the two enantiomers of **G1** with very similar binding constants, but **36** prefers the R-enantiomer by a factor of 2.2. However, the chiral recognition by  $^1\text{H}$  NMR spectral studies could not be easily achieved because the host-guest binding does not change the macrocycle proton signal. Later, the authors introduced ester groups into glycolurils [53] to produce the ester functionalized **37** and **38** (Figure 14), which could affect binding preference by changing the spatial constraints of substituents.

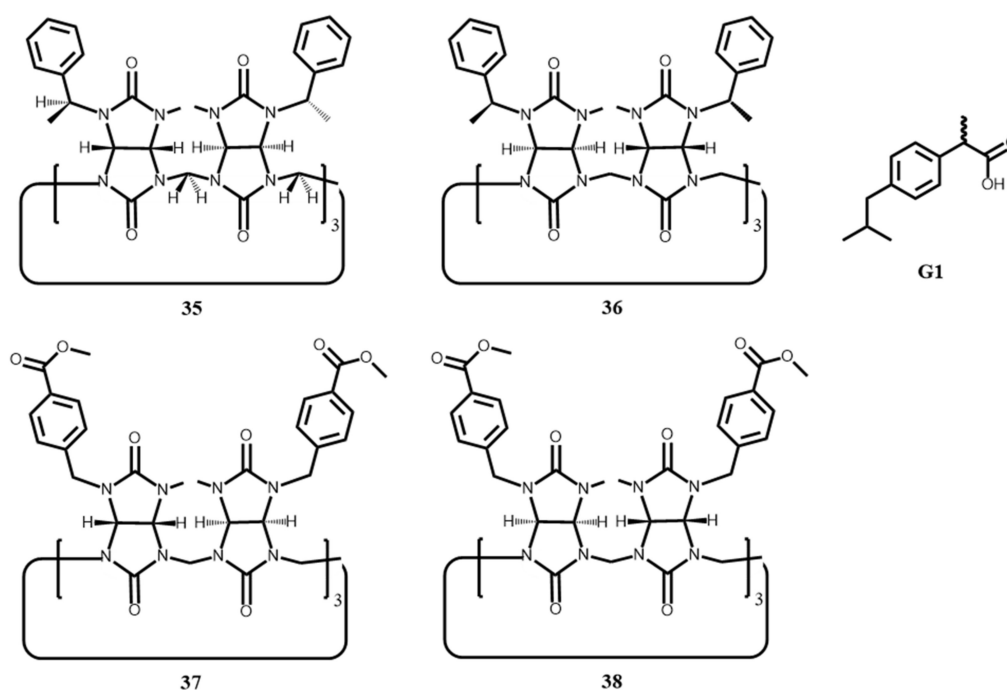


**Figure 14.** The chemical structure of chiral bambusurils.

### 3.4. Other Chiral Macrocyclic Compounds

Calixarenes are a class of bowl-shaped macrocycles with versatile functions, relatively rigid frameworks, and easy chemical derivatization. Tiefenbacher and co-workers reported [54] the multistep synthesis of a class of inherent chiral calixarenes (Figure 15). The pair of enantiomers of *M*-(-)-**39** and *P*-(+)-**39** were successfully separated by HPLC, which exhibited mirror-symmetric CD signals. The binding behavior of these chiral calixarenes with organic amines has been studied in acetone, and it was demonstrated that the binding affinity of ( $\pm$ )-**39** to the guest was relatively strong. The complexation of *M*-(-)-**39** and *P*-(+)-**39** with the chiral guest molecule *R*-**G8** showed a difference of 1:1.48, demonstrating that this chiral macrocyclic molecule has an excellent chiral recognition ability for chiral amine.

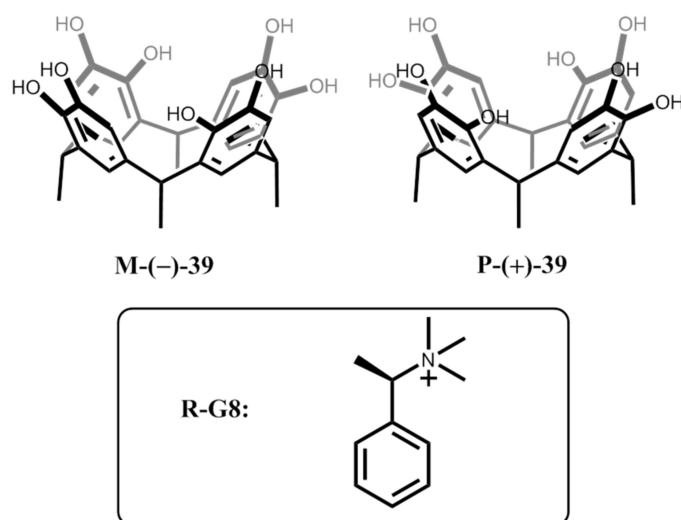


**Figure 15.** The chemical structure of *R-G8* and **39**.

Studies have recently been carried out on the application of calixarenes to electrochemical or macroscopic chiral devices by taking advantage of their good chiral recognition characteristics [55–57]. For example, Li and co-workers proposed [57] a new strategy to modify calix[4]arene into nanostructured surfaces through self-assembly, and chiral selective interaction with glucose was investigated by measuring contact angles of functional surfaces. Yang and co-workers have investigated chiral recognition with pillar[5]arene molecular universal joint-coordinated ruthenium complex by electrochemiluminescence detection, which showed significant discrimination for tryptophan [23].

Cyclodextrins are inherently chiral macrocyclic molecules that show antidifferentiation in photoreactions and supramolecular complexation [58–61]. Yang and co-workers have proposed an intriguing strategy to construct chiral cavities by implanting an achiral axis into the large chiral cavity of  $\gamma$ -cyclodextrin through rotaxanation [62–65]. The implanting aromatic axis plays the role of a spacer that changes the round shape of native cyclodextrin and provides  $\pi$ – $\pi$  interaction with the incoming chiral guest. The rotaxane thus constructed could enhance the enantioselectivity of sensitized photoisomerization of cyclooctadiene [62]. Moreover, a pair of enantiomeric amines entered into the residue space of cyclodextrin showed separated NMR signals due to the different binding affinities with the rotaxane and varied orientation in the cavity [63].

Chiral macrocyclic molecules can enantioselectively recognize chiral molecules based on the different binding affinities corresponding to the chiral enantiomers and/or the differences in spectral response of the host-guest complex. Zheng et al. have studied [66] chiral tetraphenylethylene (TPE)-based macrocycles with optically pure compounds that could identify two enantiomers of chiral acids and  $\alpha$ -amino acids by enantioselective aggregation and the consequent AIE effect. The enantiodifferentiation of different chiral macrocyclic compounds is summarized in Table 2.

**Table 2.** The targeted substrates, binding constants ( $K_a$ ), and highest ratios of enantiodifferentiation obtained with chiral macrocyclic chiral sensors.

Chiral Macrocycle	Targeted Substrate	$K_a/M^{-1}$	$K_R/K_S$ or $K_L/K_D$
27–30	Carboxylates	$10^4\sim 10^6$	2.25/1 for <b>S-27</b> (KTP) 1/3.88 for <b>S-28</b> (IBP) 1/20 for <b>S-29</b> (PPA) 20/1 for <b>S-30</b> (PPA)
31 and 32	Octyl glycosides	$10^4\sim 10^5$	1/2.61 for <b>S-31</b> 1.1/1 for <b>S-32</b> (oct- $\beta$ -Fru)
33	Trimethylamine derivatives	$10^2\sim 10^3$	4.91/1 for <b>P-33</b> 1/6.67 for <b>M-33</b> (methylated derivative of 1-indamine)
35	Carboxylic acids	$10^3$	1/3.2 ( $\alpha$ -methoxy-phenylacetic)
36	Carboxylic acids	$10^3$	1/2.7 (ibuprofen)
37	Carboxylic acids	$10^3\sim 10^4$	2.0/1 (N-acetyl leucine)

#### 4. Conclusions

In summary, macrocyclic hosts-based supramolecular chiral sensing has shown significant progress in recent years. Chemical sensors suitable for chiral sensing generally comprise an interaction component and a signal output component, differentiating chiral analytes by interacting affinity or spectral response. Macrocyclic compounds could play the role of host molecule without the introduction of additional interacting components. By virtue of the unique cavity of the macrocyclic compounds, various non-covalent interactions, including hydrophobic/hydrophilic interactions, electricity-rich/deficient interactions, electrostatic interactions, hydrogen bonding,  $\pi$ - $\pi$  interactions, and Van der Waals interactions, could work to include various types of chiral guest molecules. On the other hand, macrocyclic chiral sensors are usually composed of aromatic subunits. The complexation with a chiral guest could cause conformational change/preference, leading to a significant response of chiroptical spectra. Chemically grafting additional interacting functional groups or chromophores could improve the complexation affinity/spectral response or extend the detecting wavelength. For chiral hosts, the chirality sensing/discrimination could apply non-chiroptical methods, such as UV-vis, fluorescence, and NMR spectroscopies. The diversity of structural frameworks and macrocyclic compounds provides versatile opportunities for chirality sensing. Multiple interactions and even hierarchical chiral structures provide more possibilities for signal amplification. New macrocyclic arenes, such as naphthalene-based macrocycle [67], anthracene-based macrocycle [68], phenanthracene-based macrocycle [69], and azobenzene-based macrocycle [70], have recently emerged with  $\pi$ -conjugated structures, strong luminescence properties, and flexible conformational changes. These new macrocycles provide new potential in chirality-induced CD or CPL detection. Chiral sensing with macrocyclic compounds has made fast progress.

However, challenges still remain and need further attention in future research. Currently, chirality sensing with macrocyclic molecules have demonstrated success in chiral sensing or recognition of chiral guest molecules with certain functional groups, such as amines, alcohols, or carboxylic acids. The scope of chiral guests is still limited and needs to be expanded. In order to obtain a good sensing effect, it is generally required that the chiral center not be far away from the functional group; this greatly limits the application of macrocyclic sensors. The development of supramolecular macrocycles applicable to a wider range of chiral substrates with highly efficient binding and effective chiral trans-

fer deserves further efforts, particularly in the design and synthesis of more macrocyclic macromolecules. Breakthroughs in this research area could originate from diverse aspects, including designing and synthesizing host molecules with specific binding ability, synthesizing water-soluble macrocyclic molecules to enhance their applicability, improving the enantioselective recognition ability of hosts, and enhancing the chiroptical response during the chiral induction by introducing chromophores having absorption at longer wavelength regions. With further exploration, chemists will surely develop more sensitive, fast, and effective macrocyclic chiral sensors that can facilitate the development of chiral analysis techniques and other chiral research fields.

**Author Contributions:** Conceptualization, X.L., W.W., H.W. and C.Y.; writing—review and editing, X.L., W.L., P.J. and C.Y.; All authors have read and agreed to the published version of the manuscript.

**Funding:** This research was funded by the National Natural Science Foundation of China (Nos. 92056116, 21871194, 21971169), The Fundamental Research Funds for the Central Universities (20826041D4117), and the Comprehensive Training Platform of Specialized Laboratory, College of Chemistry.

**Institutional Review Board Statement:** Not applicable.

**Informed Consent Statement:** Not applicable.

**Data Availability Statement:** Not applicable.

**Acknowledgments:** We are thankful for the financial support from National Natural Science Foundation of China and The Fundamental Research Funds for the Central Universities.

**Conflicts of Interest:** The authors declare no conflict of interest.

## References

1. Zhang, X.; Yin, J.; Yoon, J. Recent advances in development of chiral fluorescent and colorimetric sensors. *Chem. Rev.* **2014**, *114*, 4918–4959. [[CrossRef](#)] [[PubMed](#)]
2. Jo, H.H.; Lin, C.Y.; Anslyn, E.V. Rapid optical methods for enantiomeric excess analysis: From enantioselective indicator displacement assays to exciton-coupled circular dichroism. *Acc. Chem. Res.* **2014**, *47*, 2212–2221. [[CrossRef](#)] [[PubMed](#)]
3. Wolf, C.; Bentley, K.W. Chirality sensing using stereodynamic probes with distinct electronic circular dichroism output. *Chem. Soc. Rev.* **2013**, *42*, 5408–5424. [[CrossRef](#)] [[PubMed](#)]
4. Hembury, G.A.; Borovkov, V.V.; Inoue, Y. Chirality-Sensing Supramolecular Systems. *Chem. Rev.* **2008**, *108*, 1–73. [[CrossRef](#)]
5. Chen, Z.; Wang, Q.; Wu, X.; Li, Z.; Jiang, Y.-B. Optical chirality sensing using macrocycles, synthetic and supramolecular oligomers/polymers, and nanoparticle based sensors. *Chem. Soc. Rev.* **2015**, *44*, 4249–4263. [[CrossRef](#)]
6. Huang, S.; Yu, H.; Li, Q. Supramolecular Chirality Transfer toward Chiral Aggregation: Asymmetric Hierarchical Self-Assembly. *Adv. Sci.* **2021**, *8*, 2002132. [[CrossRef](#)]
7. Prabodh, A.; Bauer, D.; Kubik, S.; Rebmann, P.; Klärner, F.G.; Schrader, T.; Delarue Bizzini, L.; Mayor, M.; Biedermann, F. Chirality sensing of terpenes, steroids, amino acids, peptides and drugs with acyclic cucurbit[n]urils and molecular tweezers. *Chem. Commun.* **2020**, *56*, 4652–4655. [[CrossRef](#)]
8. Wang, L.L.; Quan, M.; Yang, T.L.; Chen, Z.; Jiang, W. A Green and Wide-Scope Approach for Chiroptical Sensing of Organic Molecules through Biomimetic Recognition in Water. *Angew. Chem. Int. Ed. Engl.* **2020**, *59*, 23817–23824. [[CrossRef](#)]
9. Ada, N.-H.; Nakanishi, K. *Circular Dichroic Spectroscopy: Exciton Coupling in Organic Stereochemistry*; University Science Books: Mill Valley, CA, USA, 1983.
10. Rekharsky, M.V.; Yamamura, H.; Inoue, C.; Kawai, M.; Osaka, I.; Arakawa, R.; Shiba, K.; Sato, A.; Ko, Y.H.; Selvapalam, N.; et al. Chiral Recognition in Cucurbituril Cavities. *J. Am. Chem. Soc.* **2006**, *128*, 14871–14880. [[CrossRef](#)]
11. Bailey, D.M.; Hennig, A.; Uzunova, V.D.; Nau, W.M. Supramolecular tandem enzyme assays for multiparameter sensor arrays and enantiomeric excess determination of amino acids. *Chem. Eur. J.* **2008**, *14*, 6069–6077. [[CrossRef](#)]
12. Biedermann, F.; Nau, W.M. Noncovalent chirality sensing ensembles for the detection and reaction monitoring of amino acids, peptides, proteins, and aromatic drugs. *Angew. Chem. Int. Ed. Engl.* **2014**, *53*, 5694–5699. [[CrossRef](#)]
13. Hassan, D.S.; De Los Santos, Z.A.; Brady, K.G.; Murkli, S.; Isaacs, L.; Wolf, C. Chiroptical sensing of amino acids, amines, amino alcohols, alcohols and terpenes with pi-extended acyclic cucurbiturils. *Org. Biomol. Chem.* **2021**, *19*, 4248–4253. [[CrossRef](#)]
14. Wang, L.L.; Chen, Z.; Liu, W.E.; Ke, H.; Wang, S.H.; Jiang, W. Molecular Recognition and Chirality Sensing of Epoxides in Water Using Endo-Functionalized Molecular Tubes. *J. Am. Chem. Soc.* **2017**, *139*, 8436–8439. [[CrossRef](#)]
15. Chai, H.; Chen, Z.; Wang, S.-H.; Quan, M.; Yang, L.-P.; Ke, H.; Jiang, W. Enantioselective Recognition of Neutral Molecules in Water by a Pair of Chiral Biomimetic Macrocyclic Receptors. *CCS Chem.* **2020**, *2*, 440–452. [[CrossRef](#)]

16. Huang, X.; Wang, X.; Quan, M.; Yao, H.; Ke, H.; Jiang, W. Biomimetic Recognition and Optical Sensing of Carboxylic Acids in Water by Using a Buried Salt Bridge and the Hydrophobic Effect. *Angew. Chem. Int. Ed. Engl.* **2021**, *60*, 1929–1935. [[CrossRef](#)]
17. Osawa, K.; Tagaya, H.; Kondo, S.I. Induced Circular Dichroism of Achiral Cyclic Bisurea via Hydrogen Bonds with Chiral Carboxylates. *J. Org. Chem.* **2019**, *84*, 6623–6630. [[CrossRef](#)]
18. Ogoshi, T.; Kanai, S.; Fujinami, S.; Yamagishi, T.-A.; Nakamoto, Y. para-Bridged Symmetrical Pillar[5]arenes: Their Lewis Acid Catalyzed Synthesis and Host–Guest Property. *J. Am. Chem. Soc.* **2008**, *130*, 5022–5023. [[CrossRef](#)]
19. Yao, J.; Wu, W.; Liang, W.; Feng, Y.; Zhou, D.; Chruma, J.J.; Fukuhara, G.; Mori, T.; Inoue, Y.; Yang, C. Temperature-Driven Planar Chirality Switching of a Pillar[5]arene-Based Molecular Universal Joint. *Angew. Chem. Int. Ed.* **2017**, *56*, 6869–6873. [[CrossRef](#)]
20. Xiao, C.; Wu, W.; Liang, W.; Zhou, D.; Kanagaraj, K.; Cheng, G.; Su, D.; Zhong, Z.; Chruma, J.J.; Yang, C. Redox-Triggered Chirality Switching and Guest-Capture/Release with a Pillar[6]arene-Based Molecular Universal Joint. *Angew. Chem. Int. Ed.* **2020**, *59*, 8094–8098. [[CrossRef](#)]
21. Yao, J.; Wu, W.; Xiao, C.; Su, D.; Zhong, Z.; Mori, T.; Yang, C. Overtemperature-protection intelligent molecular chiroptical photoswitches. *Nat. Commun.* **2021**, *12*, 2600. [[CrossRef](#)]
22. Fan, C.; Yao, J.; Li, G.; Guo, C.; Wu, W.; Su, D.; Zhong, Z.; Zhou, D.; Wang, Y.; Chruma, J.J.; et al. Precise Manipulation of Temperature-Driven Chirality Switching of Molecular Universal Joints through Solvent Mixing. *Chem. Eur. J.* **2019**, *25*, 12526–12537. [[CrossRef](#)]
23. Liu, C.; Yao, J.; Xiao, C.; Zhao, T.; Selvapalam, N.; Zhou, C.; Wu, W.; Yang, C. Electrochemiluminescent Chiral Discrimination with a Pillar[5]arene Molecular Universal Joint-Coordinated Ruthenium Complex. *Org. Lett.* **2021**, *23*, 3885–3890. [[CrossRef](#)]
24. Xiao, C.; Liang, W.; Wu, W.; Kanagaraj, K.; Yang, Y.; Wen, K.; Yang, C. Resolution and Racemization of a Planar-Chiral A1/A2-Disubstituted Pillar[5]arene. *Symmetry* **2019**, *11*, 773. [[CrossRef](#)]
25. Li, G.; Fan, C.; Cheng, G.; Wu, W.; Yang, C. Synthesis, enantioseparation and photophysical properties of planar-chiral pillar[5]arene derivatives bearing fluorophore fragments. *Beilstein J. Org. Chem.* **2019**, *15*, 1601–1611. [[CrossRef](#)]
26. Yao, J.; Mizuno, H.; Xiao, C.; Wu, W.; Inoue, Y.; Yang, C.; Fukuhara, G. Pressure-driven, solvation-directed planar chirality switching of cyclophano-pillar[5]arenes (molecular universal joints). *Chem. Sci.* **2021**, *12*, 4361–4366. [[CrossRef](#)]
27. Ji, J.; Li, Y.; Xiao, C.; Cheng, G.; Luo, K.; Gong, Q.; Zhou, D.; Chruma, J.J.; Wu, W.; Yang, C. Supramolecular enantiomeric and structural differentiation of amino acid derivatives with achiral pillar[5]arene homologs. *Chem. Commun.* **2020**, *56*, 161–164. [[CrossRef](#)]
28. Zhu, H.; Li, Q.; Gao, Z.; Wang, H.; Shi, B.; Wu, Y.; Shangguan, L.; Hong, X.; Wang, F.; Huang, F. Pillararene Host–Guest Complexation Induced Chirality Amplification: A New Way to Detect Cryptochiral Compounds. *Angew. Chem. Int. Ed. Engl.* **2020**, *59*, 10868–10872. [[CrossRef](#)]
29. Chen, Y.; Fu, L.; Sun, B.; Qian, C.; Wang, R.; Jiang, J.; Lin, C.; Ma, J.; Wang, L. Competitive Selection of Conformation Chirality of Water-Soluble Pillar[5]arene Induced by Amino Acid Derivatives. *Org. Lett.* **2020**, *22*, 2266–2270. [[CrossRef](#)]
30. Chen, Y.; Fu, L.; Sun, B.; Qian, C.; Pangannaya, S.; Zhu, H.; Ma, J.; Jiang, J.; Ni, Z.; Wang, R.; et al. Selection of Planar Chiral Conformations between Pillar[5,6]arenes Induced by Amino Acid Derivatives in Aqueous Media. *Chem. Eur. J.* **2021**, *27*, 5890–5896. [[CrossRef](#)]
31. Fa, S.; Egami, K.; Adachi, K.; Kato, K.; Ogoshi, T. Sequential Chiral Induction and Regulator-Assisted Chiral Memory of Pillar[5]arenes. *Angew. Chem. Int. Ed. Engl.* **2020**, *59*, 20353–20356. [[CrossRef](#)]
32. Setsune, J.; Tsukajima, A.; Okazaki, N.; Lintuluoto, J.M.; Lintuluoto, M. Enantioselective induction of helical chirality in cyclooctapyrroles by metal-complex formation. *Angew. Chem. Int. Ed. Engl.* **2009**, *48*, 771–775. [[CrossRef](#)] [[PubMed](#)]
33. Ie, M.; Setsune, J.-I.; Eda, K.; Tsuda, A. Chiroptical sensing of oligonucleotides with a cyclic octapyrrole. *Org. Chem. Front.* **2015**, *2*, 29–33. [[CrossRef](#)]
34. Xiong, J.B.; Feng, H.T.; Sun, J.P.; Xie, W.Z.; Yang, D.; Liu, M.; Zheng, Y.S. The Fixed Propeller-Like Conformation of Tetraphenylethylene that Reveals Aggregation-Induced Emission Effect, Chiral Recognition, and Enhanced Chiroptical Property. *J. Am. Chem. Soc.* **2016**, *138*, 11469–11472. [[CrossRef](#)] [[PubMed](#)]
35. Zhang, H.; Cheng, L.; Nian, H.; Du, J.; Chen, T.; Cao, L. Adaptive chirality of achiral tetraphenylethylene-based tetracationic cyclophanes with dual responses of fluorescence and circular dichroism in water. *Chem. Commun.* **2021**, *57*, 3135–3138. [[CrossRef](#)]
36. Cheng, L.; Liu, K.; Duan, Y.; Duan, H.; Li, Y.; Gao, M.; Cao, L. Adaptive Chirality of an Achiral Cage: Chirality Transfer, Induction, and Circularly Polarized Luminescence through Aqueous Host–Guest Complexation. *CCS Chem.* **2020**, 2749–2751. [[CrossRef](#)]
37. Sapotta, M.; Spent, P.; Saha-Möller, C.R.; Würthner, F. Guest-mediated chirality transfer in the host–guest complexes of an atropisomeric perylene bisimide cyclophane host. *Org. Chem. Front.* **2019**, *6*, 892–899. [[CrossRef](#)]
38. Nian, H.; Cheng, L.; Wang, L.; Zhang, H.; Wang, P.; Li, Y.; Cao, L. Hierarchical Two-Level Supramolecular Chirality of an Achiral Anthracene-Based Tetracationic Nanotube in Water. *Angew. Chem. Int. Ed. Engl.* **2021**, *133*, 15482–15486. [[CrossRef](#)]
39. Weirich, L.; Merten, C. Induced VCD and conformational chirality in host–guest complexes of a chiral ammonium salt with crown ethers. *Phys. Chem. Chem. Phys.* **2021**, *23*, 18300–18307. [[CrossRef](#)]
40. Liu, H.L.; Hou, X.L.; Pu, L. Enantioselective precipitation and solid-state fluorescence enhancement in the recognition of alpha-hydroxycarboxylic acids. *Angew. Chem. Int. Ed. Engl.* **2009**, *48*, 382–385. [[CrossRef](#)]
41. Yu, S.; Pu, L. Pseudoenantiomeric Fluorescent Sensors in a Chiral Assay. *J. Am. Chem. Soc.* **2010**, *132*, 17698–17700. [[CrossRef](#)]
42. Akdeniz, A.; Minami, T.; Watanabe, S.; Yokoyama, M.; Ema, T.; Anzenbacher, P., Jr. Determination of enantiomeric excess of carboxylates by fluorescent macrocyclic sensors. *Chem. Sci.* **2016**, *7*, 2016–2022. [[CrossRef](#)]

43. Tyszka-Gumkowska, A.; Pikus, G.; Jurczak, J. Chiral Recognition of Carboxylate Anions by (R)-BINOL-Based Macrocyclic Receptors. *Molecules* **2019**, *24*, 2635. [[CrossRef](#)]
44. Abe, H.; Yoneda, T.; Ohishi, Y.; Inouye, M. D3h-Symmetrical Shape-Persistent Macrocycles Consisting of Pyridine-Acetylene-Phenol Conjugates as an Efficient Host Architecture for Saccharide Recognition. *Chem. Eur. J.* **2016**, *22*, 18944–18952. [[CrossRef](#)]
45. Lim, J.Y.C.; Marques, I.; Felix, V.; Beer, P.D. Enantioselective Anion Recognition by Chiral Halogen-Bonding [2]Rotaxanes. *J. Am. Chem. Soc.* **2017**, *139*, 12228–12239. [[CrossRef](#)]
46. Ohishi, Y.; Murase, M.; Abe, H.; Inouye, M. Enantioselective Solid-Liquid Extraction of Native Saccharides with Chiral BINOL-Based Pyridine-Phenol Type Macrocycles. *Org. Lett.* **2019**, *21*, 6202–6207. [[CrossRef](#)]
47. Zhang, G.W.; Li, P.F.; Meng, Z.; Wang, H.X.; Han, Y.; Chen, C.F. Triptycene-Based Chiral Macrocyclic Hosts for Highly Enantioselective Recognition of Chiral Guests Containing a Trimethylamino Group. *Angew. Chem. Int. Ed. Engl.* **2016**, *55*, 5304–5308. [[CrossRef](#)]
48. Guo, Y.; Han, Y.; Chen, C.F. Construction of Chiral Nanoassemblies Based on Host-Guest Complexes and Their Responsive CD and CPL Properties: Chirality Transfer From 2,6-helic[6]arenes to a Stilbazolium Derivative. *Front. Chem.* **2019**, *7*, 543. [[CrossRef](#)]
49. Li, J.; Han, Y.; Chen, C.F. Synthesis of Chiral Helic[1]triptycene[3]arenes and Their Enantioselective Recognition Towards Chiral Guests Containing Aminoindan Groups. *Molecules* **2021**, *26*, 536. [[CrossRef](#)]
50. Lisbjerg, M.; Jessen, B.M.; Rasmussen, B.; Nielsen, B.E.; Madsen, A.Ø.; Pittelkow, M. Discovery of a cyclic 6 + 6 hexamer of d-biotin and formaldehyde. *Chem. Sci.* **2014**, *5*, 2647–2650. [[CrossRef](#)]
51. Aav, R.; Shmatova, E.; Reile, I.; Borissova, M.; Topić, F.; Rissanen, K. New Chiral Cyclohexylhemicucurbit[6]uril. *Org. Lett.* **2013**, *15*, 3786–3789. [[CrossRef](#)]
52. Sokolov, J.; Sindelar, V. Chiral Bambusurils for Enantioselective Recognition of Carboxylate Anion Guests. *Chem. Eur. J.* **2018**, *24*, 15482–15485. [[CrossRef](#)]
53. Sokolov, J.; Stefek, A.; Sindelar, V. Functionalized Chiral Bambusurils: Synthesis and Host-Guest Interactions with Chiral Carboxylates. *Chempluschem* **2020**, *85*, 1307–1314. [[CrossRef](#)]
54. Nemat, S.J.; Jedrzejewska, H.; Prescimone, A.; Szumna, A.; Tiefenbacher, K. Catechol[4]arene: The Missing Chiral Member of the Calix[4]arene Family. *Org. Lett.* **2020**, *22*, 5506–5510. [[CrossRef](#)]
55. Quan, J.; Nie, G.; Xue, H.; Luo, L.; Zhang, R.; Li, H. Macroscopic Chiral Recognition by Calix[4]arene-Based Host-Guest Interactions. *Chem. Eur. J.* **2018**, *24*, 15502–15506. [[CrossRef](#)]
56. Zhang, W.-Z.; Ma, H.; Xiang, G.-Y.; Luo, J.; Chung, W.-S. Calix[4]arenes with Combined Axial Chirality and Inherent Chirality: Synthesis, Absolute Configuration and Chiral Recognition. *ChemistrySelect* **2016**, *1*, 2486–2491. [[CrossRef](#)]
57. Sun, Y.; Mei, Y.; Quan, J.; Xiao, X.; Zhang, L.; Tian, D.; Li, H. The macroscopic wettable surface: Fabricated by calix[4]arene-based host-guest interaction and chiral discrimination of glucose. *Chem. Commun.* **2016**, *52*, 14416–14418. [[CrossRef](#)]
58. Yang, C. Recent progress in supramolecular chiral photochemistry. *Chin. Chem. Lett.* **2013**, *24*, 437–441. [[CrossRef](#)]
59. Yang, C.; Inoue, Y. Supramolecular photochirogenesis. *Chem. Soc. Rev.* **2014**, *43*, 4123–4143. [[CrossRef](#)] [[PubMed](#)]
60. Ji, J.; Wu, W.; Liang, W.; Cheng, G.; Matsushita, R.; Yan, Z.; Wei, X.; Rao, M.; Yuan, D.-Q.; Fukuhara, G.; et al. An Ultimate Stereocontrol in Supramolecular Photochirogenesis: Photocyclodimerization of 2-Anthracenecarboxylate Mediated by Sulfur-Linked  $\beta$ -Cyclodextrin Dimers. *J. Am. Chem. Soc.* **2019**, *141*, 9225–9238. [[CrossRef](#)] [[PubMed](#)]
61. Ji, J.; Wu, W.; Wei, X.; Rao, M.; Zhou, D.; Cheng, G.; Gong, Q.; Luo, K.; Yang, C. Synergetic effects in the enantiodifferentiating photocyclodimerization of 2-anthracenecarboxylic acid mediated by  $\beta$ -cyclodextrin-pillar[5]arene-hybridized hosts. *Chem. Commun.* **2020**, *56*, 6197–6200. [[CrossRef](#)] [[PubMed](#)]
62. Yan, Z.; Huang, Q.; Liang, W.; Yu, X.; Zhou, D.; Wu, W.; Chruma, J.J.; Yang, C. Enantiodifferentiation in the Photoisomerization of (Z,Z)-1,3-Cyclooctadiene in the Cavity of  $\gamma$ -Cyclodextrin-Cucurbit[6]uril-Wheeled [4]Rotaxanes with an Encapsulated Photosensitizer. *Org. Lett.* **2017**, *19*, 898–901. [[CrossRef](#)]
63. Dai, L.; Wu, W.; Liang, W.; Chen, W.; Yu, X.; Ji, J.; Xiao, C.; Yang, C. Enhanced chiral recognition by  $\gamma$ -cyclodextrin-cucurbit[6]uril-cowheeled [4]pseudorotaxanes. *Chem. Commun.* **2018**, *54*, 2643–2646. [[CrossRef](#)]
64. Yu, X.; Liang, W.; Huang, Q.; Wu, W.; Chruma, J.J.; Yang, C. Room-temperature phosphorescent  $\gamma$ -cyclodextrin-cucurbit[6]uril-cowheeled [4]rotaxanes for specific sensing of tryptophan. *Chem. Commun.* **2019**, *55*, 3156–3159. [[CrossRef](#)]
65. Liu, R.; Zhang, Y.; Wu, W.; Liang, W.; Huang, Q.; Yu, X.; Xu, W.; Zhou, D.; Selvapalam, N.; Yang, C. Temperature-driven braking of  $\gamma$ -cyclodextrin-cucurbit[6]uril-cowheeled [4]rotaxanes. *Chin. Chem. Lett.* **2019**, *30*, 577–581. [[CrossRef](#)]
66. Feng, H.T.; Zhang, X.; Zheng, Y.S. Fluorescence Turn-on Enantioselective Recognition of both Chiral Acidic Compounds and alpha-Amino Acids by a Chiral Tetraphenylethylene Macrocycle Amine. *J. Org. Chem.* **2015**, *80*, 8096–8101. [[CrossRef](#)]
67. Della Sala, P.; Del Regno, R.; Talotta, C.; Capobianco, A.; Hickey, N.; Geremia, S.; De Rosa, M.; Spinella, A.; Soriente, A.; Neri, P.; et al. Prismarenes: A New Class of Macrocyclic Hosts Obtained by Templatation in a Thermodynamically Controlled Synthesis. *J. Am. Chem. Soc.* **2020**, *142*, 1752–1756. [[CrossRef](#)]
68. Han, X.N.; Han, Y.; Chen, C.F. Pagoda[4]arene and i-Pagoda[4]arene. *J. Am. Chem. Soc.* **2020**, *142*, 8262–8269. [[CrossRef](#)]
69. Wang, J.; Ju, Y.Y.; Low, K.H.; Tan, Y.Z.; Liu, J. A Molecular Transformer: A pi-Conjugated Macrocycle as an Adaptable Host. *Angew. Chem. Int. Ed. Engl.* **2021**, *60*, 11814–11818. [[CrossRef](#)]
70. Liu, Y.; Wang, H.; Shangguan, L.; Liu, P.; Shi, B.; Hong, X.; Huang, F. Selective Separation of Phenanthrene from Aromatic Isomer Mixtures by a Water-Soluble Azobenzene-Based Macrocycle. *J. Am. Chem. Soc.* **2021**, *143*, 3081–3085. [[CrossRef](#)]